

A UNIFIED NEAR-INFRARED SPECTRAL CLASSIFICATION SCHEME FOR T DWARFS

ADAM J. BURGASSER,^{1,2} T. R. GEBALLE,³ S. K. LEGGETT,⁴ J. DAVY KIRKPATRICK,⁵ AND DAVID A. GOLIMOWSKI⁶

Received 2005 June 18; accepted 2005 October 3

ABSTRACT

A revised near-infrared classification scheme for T dwarfs is presented, based on and superseding prior schemes developed by Burgasser and coworkers and Geballe and coworkers, and defined following the precepts of the MK process. Drawing from two large spectroscopic libraries of T dwarfs identified largely in the Sloan Digital Sky Survey and the Two Micron All Sky Survey, nine primary spectral standards and five alternate standards spanning spectral types T0–T8 are identified that match criteria of spectral character, brightness, absence of a resolved companion, and accessibility from both the Northern and Southern Hemispheres. The classification of T dwarfs is formally made by the direct comparison of near-infrared spectral data of equivalent resolution to the spectra of these standards. Alternately, we have redefined five key spectral indices measuring the strengths of the major H₂O and CH₄ bands in the 1–2.5 μ m region that may be used as a proxy to direct spectral comparison. Two methods of determining T spectral type using these indices are outlined and yield equivalent results. These classifications are also equivalent to those from prior schemes, implying that no revision of existing spectral type trends is required. The one-dimensional scheme presented here provides a first step toward the observational characterization of the lowest luminosity brown dwarfs currently known. Future extensions to incorporate spectral variations arising from differences in photospheric dust content, gravity, and metallicity are briefly discussed. A compendium of all currently known T dwarfs with updated classifications is presented.

Subject headings: stars: fundamental parameters — stars: low-mass, brown dwarfs

Online material: machine-readable table

1. INTRODUCTION

Classification is an important first step in all fields of empirical natural science, from biology (e.g., the taxonomy of species; Linnaeus 1735) to chemistry (e.g., the periodic table of elements; Mendeleev 1869) to several subfields of astronomy (e.g., the Hubble sequence of galaxies; Hubble 1936). The identification and quantification of similarities and differences in observed phenomena help to clarify their governing mechanisms, while providing a standard framework for our continually evolving theoretical understanding.

In stellar astronomy, spectral classification has been and remains a powerful tool, providing insight into the physical characteristics of stars and stellar populations and enabling the study of Galactic structure (e.g., Morgan et al. 1952). From the first stellar spectral groups designated by Secchi (1866), the classification of stars has evolved in complexity and breadth, largely due to advances in technology and the compilation of large spectral catalogs (e.g., the Henry Draper [HD] catalog; Cannon & Pickering 1918a, 1918b, 1919a, 1919b, 1920, 1921, 1922, 1923, 1924). Nevertheless, nearly all existing stellar classification schemes remain observationally based. The most successful follow the MK process (Morgan et al. 1943; Morgan & Keenan 1973; Keenan &

McNeil 1976; Morgan et al. 1978; Garrison 1984; Corbally et al. 1994), a method by which stellar classes are defined by specific standard stars, and all other stars are classified by the direct comparison of spectra over a designated wavelength range and resolution. This method allows spectral classifications to remain independent of physical interpretations, concepts that can evolve even as the spectra themselves generally do not. Examples of MK classification schemes include the Michigan Catalogue of Spectral Types for the HD stars (Houk & Cowley 1975; Houk 1978, 1982; Houk & Smith-Moore 1988; Houk & Swift 1999), automated classifications through neural network techniques (e.g., von Hippel et al. 1994; Bailer-Jones et al. 1998), and classification schemes of normal stars at UV (e.g., Rountree & Sonneborn 1991) and near-infrared (NIR; e.g., Wallace & Hinkle 1997) wavelengths.

Recently, two new spectral classes of low-mass stars and brown dwarfs (stars with insufficient mass to sustain hydrogen fusion; Kumar 1962; Hayashi & Nakano 1963) have been identified. These sources, the L dwarfs (Kirkpatrick et al. 1999; Martín et al. 1999) and the T dwarfs (Burgasser et al. 2002b, hereafter B02; Geballe et al. 2002, hereafter G02), lie beyond the standard stellar main sequence. L dwarfs exhibit optical spectra with waning TiO and VO bands (characteristic of M dwarfs); strengthening metal hydride, alkali, and H₂O absorption features; and increasingly red optical/NIR spectral energy distributions. T dwarfs (Fig. 1) are distinguished by the presence of CH₄ absorption in their NIR spectra, a species generally found in planetary atmospheres (Geballe et al. 1996), as well as pressure-broadened alkali resonance lines in the optical, strong H₂O bands, and collision-induced H₂ absorption (Saumon et al. 1994; Borysow et al. 1997) suppressing flux at 2 μ m. The sequence of spectral types from M to L to T is largely one of decreasing effective temperature and luminosity (Dahn et al. 2002; Vrba et al. 2004; Golimowski et al. 2004; however, see § 5.1) and as such is a natural extension of the stellar main sequence.

¹ Department of Astrophysics, Division of Physical Sciences, American Museum of Natural History, Central Park West at 79th Street, New York, NY 10024; currently at Massachusetts Institute of Technology, Kavli Institute for Astrophysics and Space Research, Building 37-664B, 77 Massachusetts Avenue, Cambridge, MA 02139; ajb@mit.edu.

² Spitzer Fellow.

³ Gemini Observatory, 670 North A’ohoku Place, Hilo, HI 96720.

⁴ Joint Astronomy Centre, 660 North A’ohoku Place, Hilo, HI 96720.

⁵ Infrared Processing and Analysis Center, M/S 100-22, California Institute of Technology, Pasadena, CA 91125.

⁶ Department of Physics and Astronomy, Johns Hopkins University, 3701 San Martin Drive, Baltimore, MD 21218.

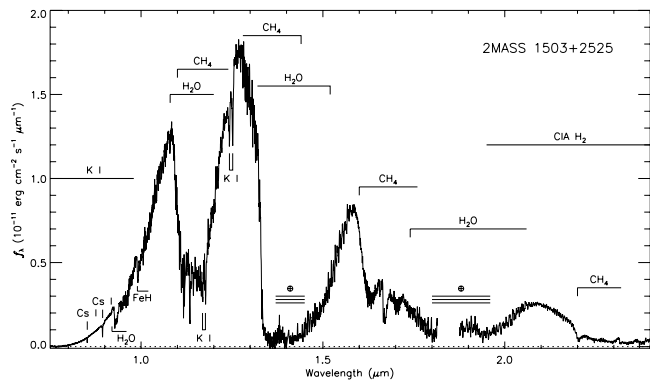


Fig. 1.—The 0.75–2.5 μm spectrum of the T5 spectral standard 2MASS 1503+2525 observed at a spectral resolution $\lambda/\Delta\lambda \sim 1200$ (Burgasser et al. 2003b, 2004). Defining features of T dwarf NIR spectra are labeled.

Initial spectral classification schemes for the colder of these two classes, the T dwarfs, have been proposed independently by B02 and G02. Both are defined in the 1–2.5 μm spectral window where T dwarfs emit the majority of their flux (e.g., Allard et al. 2001). The underlying philosophies of these two schemes are somewhat different, however. B02 identified seven representative standards spanning types T1–T8 (excluding subtype T4) and classified a sizeable but inhomogeneous sample of low- and moderate-resolution spectra by the comparison of a set of spectral indices. G02 analyzed a smaller but homogenous sample of $\lambda/\Delta\lambda \sim 400$ NIR spectra and also determined classifications using spectral indices, but no standards were explicitly defined.

Neither of these schemes adheres rigorously to the MK process; yet, despite their underlying differences, classifications differ by no more than 0.5 subtypes (Burgasser et al. 2003a). On the other hand, the existence of two separate classification schemes for T dwarfs has led to redundancies and confusion in the literature (e.g., Scholz et al. 2003). Furthermore, the relatively few T dwarfs (roughly 30) known at the time these schemes were introduced and the limited observations available for them resulted in an incomplete sampling of the T class and a potentially biased set of spectral standards (e.g., contaminated by peculiar sources and unresolved multiple systems). With over twice as many T dwarfs now known, primarily identified in the Sloan Digital Sky Survey (SDSS; York et al. 2000) and the Two Micron All Sky Survey (2MASS; Cutri et al. 2003), and with extensive imaging, spectroscopic, and astrometric data now available, it is an opportune time to revisit the classification of these cold brown dwarfs.

In this paper we present a revised NIR spectral classification scheme for T dwarfs that unifies and supersedes the studies of B02 and G02. This scheme is defined by a set of carefully screened spectral standard stars spanning types T0–T8 and is demonstrated on two distinct, large, and homogenous spectral samples. In § 2 we describe the primary spectral libraries employed for this study, as well as additional published data sets examined. In § 3 we identify and give detailed information on the nine primary and five alternate spectral standards used to define the sequence. In § 4 we review the methods of classifying T dwarfs, focusing first on the direct comparison of spectral data to the standard spectra as dictated by the MK process, then describing secondary methods based on redefined spectral indices sampling the major NIR H₂O and CH₄ bands. In § 5 we discuss the revised subtypes, comparing them to prior classifications. We also discuss how extensions to this one-dimensional

scheme may be made to account for secondary spectral variations, arising from physical differences in atmospheric dust content, surface gravity, and metallicity, and speculate on the end of the T dwarf class. Individual sources are discussed in § 6. Results are summarized in § 7. We provide a compendium of all presently known T dwarfs and their revised spectral types in the Appendix.

2. SPECTRAL DATA

Defining the classification of a stellar class necessitates a sizeable set of homogeneous (similar resolution and wavelength coverage) spectra for both standards and classified sources. Our study draws primarily on two large, NIR spectral libraries of T dwarfs obtained with the SpeX instrument (Rayner et al. 2003), mounted on the 3.0 m NASA Infrared Telescope Facility Telescope, and the Cooled Grating Spectrometer 4 (CGS4; Wright et al. 1993), mounted on the 3.5 m United Kingdom Infrared Telescope (UKIRT). These libraries are available in electronic form upon request.⁷

The SpeX data set is composed of prism-dispersed spectra covering 0.8–2.5 μm in a single order at a spectral resolution $\lambda/\Delta\lambda \approx 150$. These low-resolution data sufficiently sample the broad H₂O and CH₄ bands present at NIR wavelengths but cannot resolve important line features such as the 1.25 μm K I doublets (Fig. 1). The SpeX sample includes 59 spectra of 43 T dwarfs and two optically classified L8 dwarfs (Kirkpatrick et al. 1999), a subset of which have been previously published (Burgasser et al. 2004, 2005a; Cruz et al. 2004). All data have been homogeneously acquired and reduced using the Spextool package (Vacca et al. 2003; Cushing et al. 2004).

The CGS4 data set is composed of 41 spectra of 39 T dwarfs and 2 optically classified L8 dwarfs, with typical resolutions $\lambda/\Delta\lambda \approx 300$ –500.⁸ At these slightly higher resolutions, details within the molecular bands and atomic line absorptions can be resolved. The CGS4 spectra, nominally spanning 0.85–2.5 μm , require four instrumental settings to acquire, although some of the data encompass a subset of this spectral range. Nearly all of these spectra have been previously published (Geballe et al. 1996; Strauss et al. 1999; Leggett et al. 2000; Tsvetanov et al. 2000; Geballe et al. 2001; G02; Knapp et al. 2004), and data acquisition and reduction procedures can be found in the literature.

In addition to these two primary data sets, we have examined other late-type L and T dwarf spectra reported in the literature (Oppenheimer et al. 1995; Cuby et al. 1999; Burgasser et al. 2000b, 2003e; B02; Nakajima et al. 2001, 2004; Liu et al. 2002; Zapatero Osorio et al. 2002; McLean et al. 2003; McCaughrean et al. 2004; Cushing et al. 2005). As these data have been obtained with assorted instrumentation, they vary in both spectral resolution and wavelength coverage. Details of all of the spectral data sets examined here are given in Table 1.

While many of the T dwarfs with NIR spectral data have been observed by multiple instruments (e.g., 25 have been observed with both SpeX and CGS4), nearly all have had no more than two separate observations with a single instrument. The general absence of spectral monitoring observations prevents a robust analysis of spectral variability for T dwarfs and its impact on their classification. We therefore assume that the spectra are

⁷ Also see <http://DwarfArchives.org> and <http://www.jach.hawaii.edu/~skl/LTdata.html>.

⁸ With the exception of the bright T dwarf 2MASS 0559–1404, which was observed at twice this resolution (G02).

TABLE 1
SPECTRAL DATA SETS EXAMINED FOR T DWARF CLASSIFICATION

Instrument	$\lambda/\Delta\lambda$	Spectral Coverage			References
		(μm)	Number of Orders	Number of Sources	
CTIO 4 m OSIRIS.....	1200	1.1–2.4	4	20 T, 0 L	1, 2
IRTF SpeX (prism) ^a	150	0.8–2.5	1	43 T, 2 L	3, 4, 5, 6
IRTF SpeX (SXD).....	1200	0.9–2.5	4–6	8 T, 1 L	3, 7
Keck NIRC.....	100	0.9–2.5	1–2	17 T, 0 L	1, 8, 9
Keck NIRSPEC.....	2000	Various	1–6	17 T, 2 L	10, 11
NTT ISAAC+SOFI.....	50	0.95–2.5	2	1 T, 0 L	12
Palomar 1.5 m CORMASS.....	300	0.8–2.4	4	1 T, 0 L	13
Subaru CISCO.....	500	0.9–2.5	3	2 T, 0 L	14
Subaru IRCS.....	330	1.2–2.4	3	1 T, 0 L	15
UKIRT CGS4 ^a	400	Various	1–4	39 T, 2 L	16, 17, 18, 19, 20, 21, 22
VLT NAOS-CONICA.....	1000	1.5–1.85	1	2 T, 0 L	23

NOTE.—OSIRIS (Ohio State Infrared Imager/Spectrometer): Depoy et al. (1993); SpeX: Rayner et al. (2003); NIRC (Near Infrared Camera): Matthews & Soifer (1994); NIRSPEC (Near-IR Spectrometer): McLean et al. (1998, 2000); ISAAC (Infrared Spectrometer and Array Camera): Moorwood (1997); SOFI (Son of Isaac): Moorwood et al. (1998); CORMASS (Cornell Massachusetts Slit Spectrograph): Wilson et al. (2001b); CISCO (Cooled Infrared Spectrograph and Camera for OHS): Motohara et al. (2002); IRCS (Infrared Camera and Spectrograph): Kobayashi et al. (2000); CGS4 (Cooled Grating Spectrometer 4): Wright et al. (1993); NAOS/CONICA: Lenzen et al. (1998).

^a Primary classification spectral sample.

REFERENCES.—(1) B02; (2) Burgasser et al. 2003e; (3) Burgasser et al. 2004; (4) Cruz et al. 2004; (5) Burgasser et al. 2005a; (6) A. J. Burgasser et al. 2006, in preparation; (7) Cushing et al. 2005; (8) Oppenheimer et al. 1995; (9) Zapatero Osorio et al. 2002; (10) McLean et al. 2003; (11) Liu et al. 2002; (12) Cuby et al. 1999; (13) Burgasser et al. 2000b; (14) Nakajima et al. 2004; (15) Nakajima et al. 2001; (16) Geballe et al. 1996; (17) Strauss et al. 1999; (18) Tsvetanov et al. 2000; (19) Leggett et al. 2000; (20) Geballe et al. 2001; (21) G02; (22) Knapp et al. 2004; (23) McCaughrean et al. 2004.

effectively static and representative of each source over long periods.

3. SPECTRAL STANDARDS

3.1. Primary Standards

The selection of spectral standards is the most important aspect of defining a classification scheme, as these sources provide the framework for the entire class. The set of standards should encompass the full range of spectral morphologies observed while being sufficiently unique so as to be readily distinguishable. Peculiar (e.g., unusual metallicity) or highly variable standards are poor choices as they may improperly skew the sequence. A standard that is too difficult to observe, due to its faintness, unobservable declination, or obscuration by a nearby bright star, is also of limited utility.

We have therefore attempted to select T dwarf spectral standards that conform to the following criteria: (1) reasonably bright, (2) not known to be spectroscopically peculiar (see § 6), (3) not known to be a resolved multiple system, and (4) within 25° of the celestial equator. We have considered both previously selected standards (B02) and more recently discovered sources for which extensive data (spectroscopic and otherwise) have been obtained. In this manner, nine primary standards spanning subtypes T0–T8 that best represent the known population of T dwarfs were identified. Coordinates and photometric measurements are given in Table 2; additional data are provided in the Appendix. Detailed descriptions are as follows:

*SDSS 1207+0244*⁹ (T0).—Recently identified in the SDSS by Knapp et al. (2004) and classified as T0 on the G02 scheme, this source is favored over the bright, unequal-brightness binary SDSS 0423–0414AB (G02; Burgasser et al. 2005c). No high-

resolution imaging or parallax observations have yet been made for this source.

SDSS 0837–0000 (T1).—One of the first “L/T transition objects” discovered by Leggett et al. (2000), this source was the T1 spectral standard on the B02 scheme and classified as T0.5 by G02. It is unresolved in *Hubble Space Telescope* (HST) observations (A. J. Burgasser et al. 2006, in preparation) and has a poorly constrained parallax distance of 29 ± 12 pc (Vrba et al. 2004).

SDSS 1254–0122 (T2).—Also identified by Leggett et al. (2000), this relatively bright source ($J = 14.66 \pm 0.03$; Leggett et al. 2000¹⁰) was the T2 standard in the B02 scheme and classified likewise on the G02 scheme. It is a single source in HST images (A. J. Burgasser et al. 2006, in preparation). Three parallax distance measurements have been made for SDSS 1254–0122, one in the optical (11.8 ± 0.3 pc; Dahn et al. 2002) and two in the NIR (13.7 ± 0.4 , Tinney et al. 2003; 13.2 ± 0.5 pc, Vrba et al. 2004); note the disagreement. A more precise measure is expected from the USNO NIR parallax program (F. Vrba 2005, private communication).

2MASS 1209–1004 (T3).—This recently discovered T dwarf (Burgasser et al. 2004) replaces the apparent double SDSS 1021–0304AB (A. J. Burgasser et al. 2006, in preparation) as the T3 standard on the B02 system. No high-resolution imaging or parallax measurements of this source have yet been obtained.

2MASS 2254+3123 (T4).—While outside of our declination constraint, the spectrum of this relatively bright ($J = 15.01 \pm 0.03$; Knapp et al. 2004) T dwarf fits ideally between those of our T3 and T5 standards. Identified by B02 and originally classified as T5 on that scheme (Knapp et al. [2004] classify it as T4 on the G02 scheme), it is unresolved in HST observations (A. J. Burgasser et al. 2006, in preparation). No parallax measurement has been reported for this source. Enoch et al. (2003) report a marginally significant rise of 0.5 ± 0.2 mag in the *K*-band flux of

⁹ Source designations are abbreviated in the manner SDSS hhmm±ddmm, where the suffix conforms to IAU nomenclature convention and is the sexagesimal right ascension (hours and minutes) and declination (degrees and arcminutes) at J2000.0 equinox. Full designations are provided for all known T dwarfs in the Appendix.

¹⁰ NIR photometry reported in the text is generally based on the Mauna Kea Observatory (MKO) filter system (Simons & Tokunaga 2002; Tokunaga et al. 2002), unless otherwise specified (e.g., Table 14).

TABLE 2
T DWARF SPECTRAL STANDARDS

NAME (1)	NIR SPECTRAL TYPE (2)	MKO PHOTOMETRY ^a				d^b (pc) (7)	SPECTRAL SAMPLE ^c (8)
		J (3)	$J - H$ (4)	$H - K$ (5)	$K - L'$ (6)		
Primary Standards							
SDSS J120747.17+024424.8.....	T0	15.38 ± 0.03	0.75 ± 0.04	0.47 ± 0.04	1.54 ± 0.06	...	1
SDSS J083717.21-000018.0.....	T1	16.90 ± 0.05	0.69 ± 0.07	0.23 ± 0.07	...	29 ± 12	1, 2, 3
SDSS J125453.90-012247.4.....	T2	14.66 ± 0.03	0.53 ± 0.04	0.29 ± 0.04	1.59 ± 0.06	13.7 ± 0.4	1, 2, 4, 5, 6, 7
2MASS J12095613-1004008.....	T3	15.55 ± 0.03	0.31 ± 0.04	0.07 ± 0.04	1, 2
2MASS J22541892+3123498.....	T4	15.01 ± 0.03	0.06 ± 0.04	-0.08 ± 0.04	1.79 ± 0.06	...	1, 2, 3, 5, 7
2MASS J15031961+2525196.....	T5	13.55 ± 0.03	-0.35 ± 0.04	-0.09 ± 0.04	2.08 ± 0.06	...	2, 4
SDSS J162414.37+002915.6.....	T6	15.20 ± 0.03	-0.28 ± 0.04	-0.13 ± 0.04	2.01 ± 0.05	11.00 ± 0.15	1, 2, 5, 7
2MASS J07271824+1710012.....	T7	15.19 ± 0.03	-0.48 ± 0.04	-0.02 ± 0.04	2.01 ± 0.06	9.09 ± 0.17	1, 2, 3, 5, 7
2MASS J04151954-0935066.....	T8	15.32 ± 0.03	-0.38 ± 0.04	-0.13 ± 0.04	2.55 ± 0.06	5.57 ± 0.10	1, 2, 3, 5, 7
Alternate Standards							
SDSS J042348.57-041403.5AB.....	T0	14.30 ± 0.03	0.79 ± 0.04	0.55 ± 0.04	1.51 ± 0.06	15.2 ± 0.5	1, 5, 7
SDSS J015141.69+124429.6.....	T1	16.25 ± 0.05	0.71 ± 0.07	0.36 ± 0.07	1.64 ± 0.07	21.3 ± 1.4	1, 2, 5
SDSS J102109.69-030420.1AB.....	T3	15.88 ± 0.03	0.47 ± 0.04	0.15 ± 0.04	1.62 ± 0.07	29 ± 4	1, 2, 5
2MASS J07554795+2212169.....	T5	15.46 ± 0.03	-0.24 ± 0.04	-0.16 ± 0.04	1
2MASS J15530228+1532369AB.....	T7	15.34 ± 0.03	-0.42 ± 0.04	-0.19 ± 0.04	3, 5, 7

^a MKO $JHKL'$ photometry from Strauss et al. (1999), Leggett et al. (2000, 2002b), G02, Golimowski et al. (2004), and Knapp et al. (2004).

^b Parallax measurements from Dahn et al. (2002), Tinney et al. (2003), and Vrba et al. (2004).

^c Spectral samples as follows: (1) UKIRT CGS4; (2) IRTF SpeX; (3) Keck NIRC; (4) IRTF SpeX cross-dispersed mode; (5) Keck NIRSPEC; (6) Subaru CISCO; (7) CTIO OSIRIS. See Table 1.

this object over the course of three nights, but this possible detection of variability has yet to be confirmed.

2MASS 1503+2525 (T5).—This bright source ($J = 13.55 \pm 0.03$; Knapp et al. 2004) was identified by Burgasser et al. (2003c) and originally classified as T5.5 on the B02 scheme. While at a slightly higher declination than our adopted selection criteria, the brightness of 2MASS 1503+2525 and lack of a visible companion (A. J. Burgasser et al. 2006, in preparation) make it an excellent choice as a spectral standard. No parallax distance measurement has been reported for this source.

SDSS 1624+0029 (T6).—The first known field T dwarf, identified by Strauss et al. (1999) in the SDSS database and classified as T6 on both the B02 and G02 schemes, SDSS 1624+0029 is a representative and easily accessible standard. It is unresolved in *HST* imaging observations (A. J. Burgasser et al. 2006, in preparation) and has a parallax distance measurement of 11.00 ± 0.15 pc (Tinney et al. 2003; see also Dahn et al. 2002; Vrba et al. 2004). Nakajima et al. (2000) report very low levels (1%–3%) of variability in fine H₂O features between 1.53 and 1.58 μ m in the spectrum of the source, but not significant enough to affect its gross spectral morphology.

2MASS 0727+1710 (T7).—Identified by B02 and selected as the T7 standard in that scheme (Knapp et al. [2004] classify it as T8 on the G02 scheme), this source remains an excellent spectral standard. No high-resolution imaging observations have been reported for 2MASS 0727+1710, but it has a parallax distance measurement of 9.09 ± 0.17 pc (Vrba et al. 2004).

2MASS 0415-0935 (T8).—The coldest ($T_{\text{eff}} \approx 700$ K; Vrba et al. 2004; Golimowski et al. 2004) and latest type T dwarf known, this source was initially identified by B02 and selected as the T8 standard in that scheme. It is the sole T9 on the G02 system (Knapp et al. 2004). 2MASS 0415-0935 is unresolved in *HST* imaging observations (A. J. Burgasser et al. 2006, in preparation) and is the closest (isolated) field T dwarf to the

Sun currently known, with a parallax distance measurement of 5.75 ± 0.10 pc (Vrba et al. 2004).

Figure 2 displays the spectral sequence of these standards, along with the L8 optical standard 2MASS 1632+1904 (Kirkpatrick et al. 1999), for both the SpeX and CGS4 data sets. These spectra effectively define the T dwarf class. The emergence of H -band CH₄ absorption at these spectral resolutions defines the start of the T dwarf sequence, as originally proposed by G02. Early-type T dwarfs exhibit weak CH₄ bands, strong H₂O bands, and waning CO absorption at 2.3 μ m. In later types, H₂O and CH₄ bands progressively strengthen, the 1.05, 1.25, 1.6, and 2.1 μ m peaks become more pronounced and acute, and the K -band peak becomes increasingly suppressed relative to J . The end of the T class is exemplified by the spectrum of 2MASS 0415-0935, with nearly saturated H₂O and CH₄ bands and sharp triangular flux peaks emerging between these bands. The range of spectral morphologies encompassed by the standards in Figure 2 span the full spectral variety of the currently known T dwarf population.

3.2. Alternate Standards

In addition to the primary standards, we have identified a handful of alternate standards that have nearly identical NIR spectral energy distributions but are well separated on the sky. While in some cases these sources do not strictly adhere to the constraints outlined above, their purpose is to facilitate the observation of a spectral comparator at any time of the year. The alternate standards are listed in Table 2 and described as follows:

SDSS 0423-0414AB (T0 alternate).—This relatively bright source ($J = 14.30 \pm 0.03$; Leggett et al. 2002b) was identified by G02. Its spectrum, like that of SDSS 1207+0244, exhibits exceedingly weak CH₄ absorption at H band and both CO and CH₄ bands at K band. SDSS 0423-0414AB was not selected as a primary standard here, however, as *HST* observations resolve

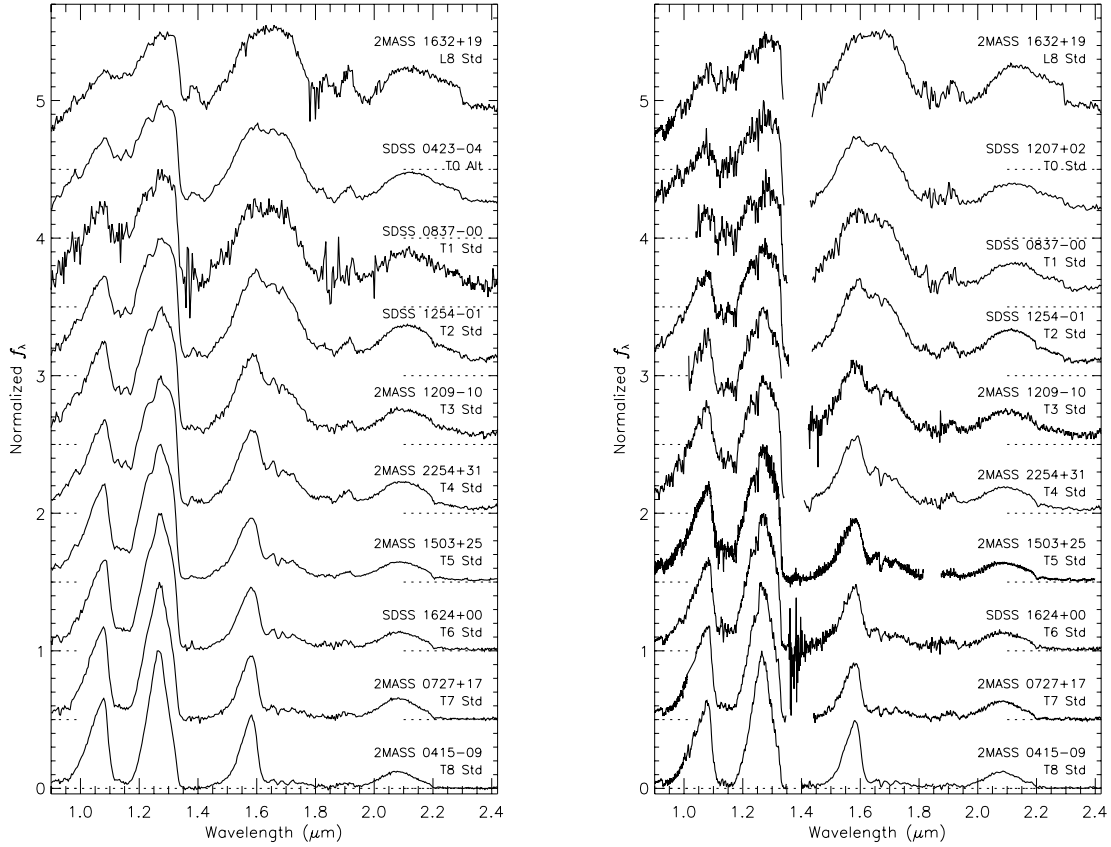


FIG. 2.—NIR spectra of T dwarf standards, along with the L8 optical standard 2MASS 1632+1904 (Kirkpatrick et al. 1999). *Left*: Low-resolution SpeX sample (note the substitution of the alternate T0 standard SDSS 0423–0414AB). *Right*: Moderate-resolution CGS4 sample (with SpeX cross-dispersed data for 2MASS 1503+2525). All spectra are normalized at 1.25 μm and offset by a constant (*dotted lines*).

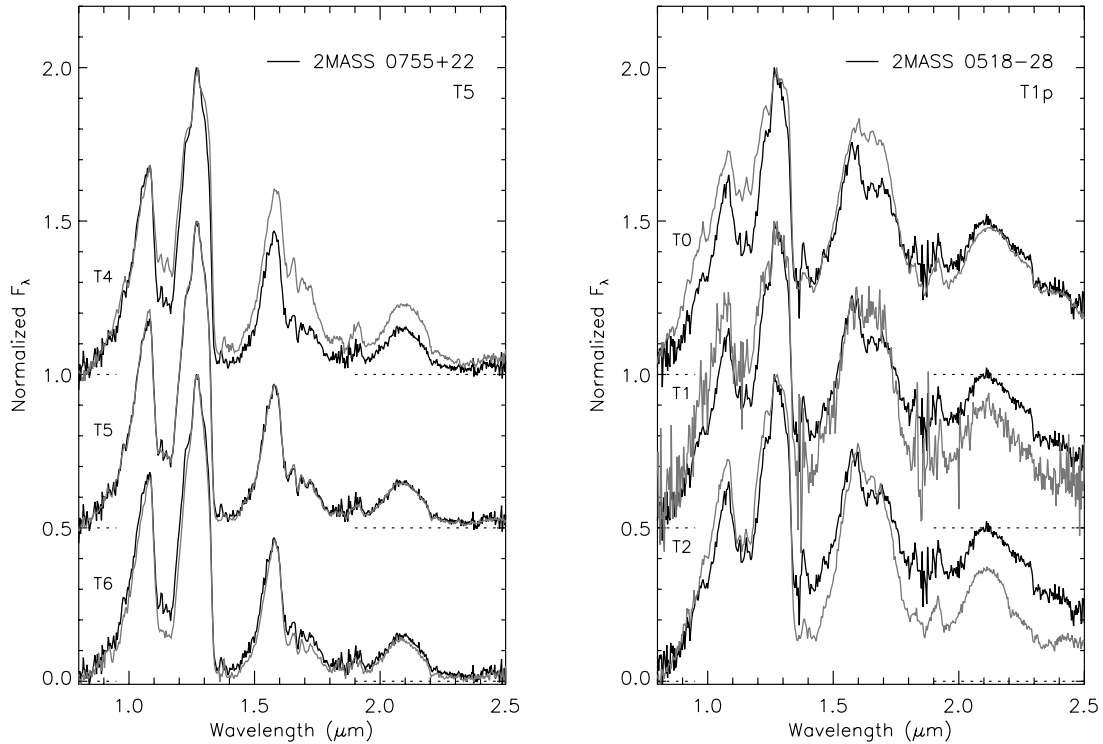


FIG. 3.—Examples of direct spectral classification for the low-resolution SpeX data. The left panel demonstrates the case of the T5 2MASS 0755+2212 (B02), which closely matches the T5 standard 2MASS 1503+2525. The right panel demonstrates the case of the peculiar T1 2MASS 0518–2828 (Cruz et al. 2004), the spectrum of which does not match any of the T dwarf standards. This source is suspected to be an unresolved L dwarf/T dwarf binary. In both panels, source (*black*) and standard (*gray*) spectra are normalized at their *J*-band flux peaks and offset by constants (*dotted lines*).

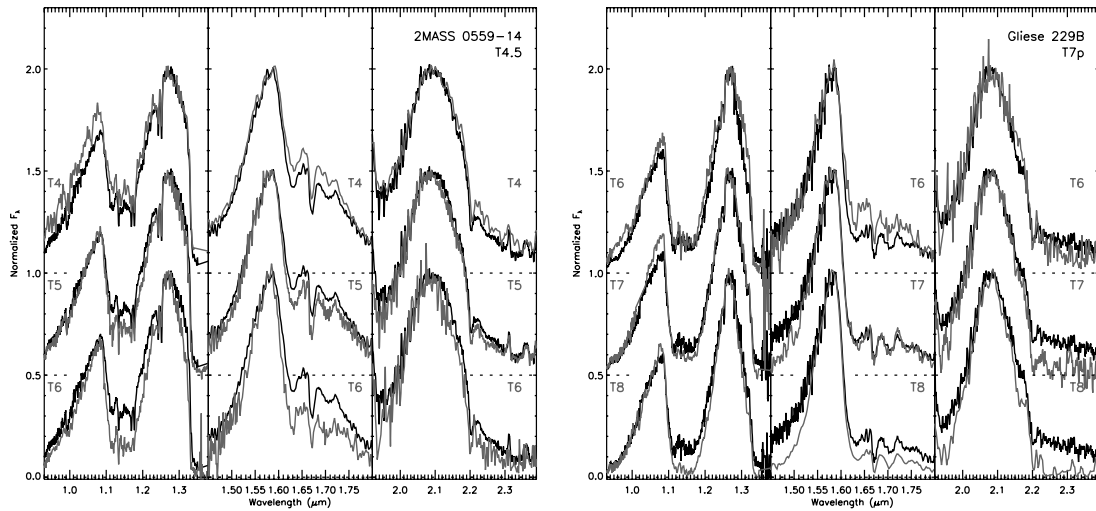


FIG. 4.—Similar to Fig. 3 for moderate-resolution CGS4 data. Here we show the examples of the T4.5 2MASS 0559–1404 and the peculiar T7 Gl 229B. Spectral data are separated into three bands, with the source (*black*) and standard (*gray*) spectra normalized at their flux peaks within the band. Note how the features in the spectrum of 2MASS 0559–1404 fall midway in strength between the T4 and T5 standard, while the spectrum of Gl 229B is inconsistent with any of the standards in all three spectral regions simultaneously.

it as an unequal-brightness binary (Burgasser et al. 2005c). Nevertheless, its NIR spectrum matches that of the T0 standard. SDSS 0423–0414AB has a parallax distance measurement of 15.2 ± 0.5 pc (Vrba et al. 2004).

SDSS 0151+1244 (T1 alternate).—Identified by G02, this faint source ($J = 16.25 \pm 0.05$; Leggett et al. 2002b) is classified as T1 on the G02 scheme. It is unresolved in *HST* images (A. J. Burgasser et al. 2006, in preparation) and has a parallax distance measurement of 21.4 ± 1.6 pc (Vrba et al. 2004). Enoch et al. (2003) report significant *K*-band variability from this source (0.42 ± 0.14 mag peak to peak) with a possible period of 2.97 hr. The faintness and apparent variability of SDSS 0151+1244 relegate it as an alternate standard, although its NIR spectrum is very similar to that of SDSS 0837–0000.

SDSS 1021–0304AB (T3 alternate).—Identified by Leggett et al. (2000) and resolved as an unequal-brightness binary in *HST* observations (A. J. Burgasser et al. 2006, in preparation), this original T3 standard on the B02 scheme (also classified as T3 by G02) remains a viable alternative to the primary standard 2MASS 1209–1004, although it is only separated by 28° on the sky. SDSS 1021–0304AB has a parallax distance measurement of 29 ± 4 pc (Tinney et al. 2003; see also Vrba et al. 2004).

2MASS 0755+2212 (T5 alternate).—Identified by B02 and classified as T5 on that system, this source has a nearly identical spectrum to that of the brighter T5 standard 2MASS 1503+2525 (Fig. 3). It is unresolved in *HST* images (A. J. Burgasser et al. 2006, in preparation). No parallax measurement has been reported.

2MASS 1553+1532AB (T7 alternate).—This late-type T dwarf identified by B02 and classified as T7 on that scheme has an NIR spectrum identical to that of the T7 primary standard 2MASS 0727+1710. Resolved into an equal-magnitude, comoving pair with *HST* and ground-based observations (A. J. Burgasser et al. 2006, in preparation), 2MASS 1553+1532AB appears to be composed of two T dwarfs with similar spectral types. No parallax measurement has been reported for this source.

4. METHODS OF CLASSIFICATION

4.1. Direct Spectral Comparison

The most straightforward and accurate means of classifying any stellar spectrum is through the direct comparison of that

spectrum to an equivalent set of spectral standards. Direct spectral comparison enables the simultaneous examination of multiple features, providing a broad match to the overall spectral morphology. Furthermore, this method facilitates the identification of peculiar sources that do not fit within the standard sequence, possibly due to secondary parameters or the presence of an unresolved companion (see § 6). Direct spectral comparison is the proscribed means of classification via the MK process (Morgan & Keenan 1973).

Spectral types for all of the T dwarfs in the SpeX and CGS4 data sets were determined by overlaying their normalized spectra onto the corresponding T dwarf standard sequences¹¹ shown in Figure 2. The standard sequences were augmented with NIR data for the L8 optical standard 2MASS 1632+1904 (Kirkpatrick et al. 1999) and for 2MASS 0310+1628 (Kirkpatrick et al. 2000), classified as L9 in the NIR by G02. Both source and standard spectra were normalized and compared in a consistent manner depending on the data set. For the low-resolution SpeX data, the entire $0.8\text{--}2.5 \mu\text{m}$ range was examined simultaneously after normalizing at the *J*-band flux peak. For the CGS4 data, spectra were separately normalized and compared in three wave bands, $0.95\text{--}1.35$, $1.45\text{--}1.8$, and $1.9\text{--}2.4 \mu\text{m}$, to minimize errors in order scaling and to discern finer details. Examples of each of these methods are shown in Figures 3 and 4.

In both cases, subtypes for individual T dwarfs were assigned according to which standard spectra provided the closest spectral match. This was gauged by the relative strengths of the major H_2O and CH_4 bands, detailed shapes of the flux peaks, and overall spectral slope. Half-subtypes were assigned for those spectra that clearly fell between standards (e.g., 2MASS 0559–1404 in Fig. 4). While this comparative technique is qualitative in nature, the distinct spectral morphologies of the standard spectra enabled unambiguous classifications in nearly all cases. As the sequence is set up in whole subtype intervals, the nominal precision of the scheme is 0.5 subtypes for reasonable

¹¹ With two exceptions: we used the alternate standard SDSS 0423–0414AB as the T0 comparator for the SpeX data set, and SpeX cross-dispersed data were used for the T5 standard 2MASS 1503+2525 in the CGS4 data set.

signal-to-noise ratio (S/N) spectra. Classifications based on low-S/N spectra are more uncertain and were specifically noted as such.

In some cases, the spectrum of a source does not fall anywhere in the standard sequence due to conflicting band strengths or substantially inconsistent broadband colors (the latter discernible with the SpeX prism data). These peculiar sources are exemplified in Figures 3 and 4 for the cases of 2MASS 0518–2828 (Cruz et al. 2004) and Gl 229B (Nakajima et al. 1995; Geballe et al. 1996), respectively. Peculiar T dwarfs were specifically labeled and are discussed in further detail in § 6.

Tables 6 and 7 (col. [9]) list the resulting subtypes as determined by direct comparison for the SpeX and CGS4 sources, respectively. Subtypes for other data reported in the literature were also determined by comparing those spectra to standards obtained at similar resolution; e.g., Keck NIRC data were compared to the SpeX standards, while Keck NIRSPEC (low resolution) data were compared to the CGS4 standards. Derived spectral types for these data are given in Tables 8–12. In all cases, the classifications of sources with multiple spectral data are identical within the scheme’s 0.5 subclass precision. The consistency of the classifications demonstrates the reliability of the direct spectral comparison technique.

4.2. Classification by Spectral Indices

In cases where one is dealing with large spectral samples or desires a quantification of deviations from the standard system (e.g., when dealing with dust or gravity effects; see § 5.2), measurements of diagnostic features through spectral indices can be useful. Such indices, typically defined as the ratio of spectral flux or flux density in two different wave bands, have had widespread use in the classification of late-type dwarfs, whose spectra typically have strong molecular and atomic features. For example, optical TiO and CaH indices defined by Reid et al. (1995) and employed by Gizis (1997) are used to segregate solar-metallicity and metal-poor M dwarfs, while NIR indices have been widely employed in the classification of M and L dwarfs (Jones et al. 1994, 1996; Delfosse et al. 1997, 1999; Tinney et al. 1998; Tokunaga & Kobayashi 1999; Reid et al. 2001; Testi et al. 2001). Both B02 and G02 make use of spectral indices in their classifications, sampling the major H₂O and CH₄ bands, the 0.8–1.0 μm red slope, color ratios, and the detailed shapes of the *J*- and *K*-band flux peaks. We revisit a subset of these indices here.

4.2.1. Revised Spectral Indices

The 1.1, 1.4, and 1.8 μm H₂O and 1.3, 1.6, and 2.2 μm CH₄ absorption bands are the most dominant and defining features of T dwarf spectra. These bands vary significantly and monotonically throughout the standard sequence and are generally correlated: strong H₂O bands are generally associated with strong CH₄ bands. These bands are also broad enough to be measured at low spectral resolutions and are found in multiple spectral regions throughout the 1.0–2.5 μm range. Because of their utility, our spectral index analysis is focused on these strong molecular features.

We reexamined the H₂O and CH₄ indices defined in B02 and G02 in order to optimize their use with T dwarf spectra. They are redefined here as the ratio of the integrated flux over a spectral window within an absorption feature to the integrated flux over the same-sized window in the neighboring pseudocontinuum. This definition minimizes large fluctuations arising from poor S/N at the bottom of strong bands (e.g., in the latest type T dwarfs).

TABLE 3
DEFINITIONS OF NEAR-INFRARED SPECTRAL INDICES

Index (1)	Numerator Range ^a (μm) (2)	Denominator Range ^a (μm) (3)	Feature (4)
H ₂ O- <i>J</i> ^b	1.140–1.165	1.260–1.285	1.15 μm H ₂ O
CH ₄ - <i>J</i> ^b	1.315–1.340	1.260–1.285	1.32 μm CH ₄
H ₂ O- <i>H</i> ^b	1.480–1.520	1.560–1.600	1.4 μm H ₂ O
CH ₄ - <i>H</i> ^b	1.635–1.675	1.560–1.600	1.65 μm CH ₄
H ₂ O- <i>K</i>	1.975–1.995	2.080–2.100	1.9 μm H ₂ O
CH ₄ - <i>K</i> ^b	2.215–2.255	2.080–2.120	2.2 μm CH ₄
<i>K/J</i>	2.060–2.100	1.250–1.290	<i>J</i> – <i>K</i> color

^a Wavelength range over which flux density (f_λ) is integrated.

^b Primary classification indices.

We also attempted to avoid regions of strong telluric absorption in order to minimize variations between spectra obtained at different sites. Finally, the spectral ratio wave bands were defined to be broad enough to facilitate use with both low and moderate spectral resolution data.

Table 3 lists the six revised classification indices, along with a seventh index measuring the ratio of flux between the *K*- and *J*-band flux peaks. This last index samples the relative strength of H₂ absorption, a gravity and metallicity-sensitive feature (e.g., B02), and is discussed in further detail in § 5.2. Figure 5 diagrams the passbands of the H₂O and CH₄ indices on the spectrum of the T5 standard 2MASS 1503+2525 and a telluric absorption spectrum typical of Mauna Kea.¹²

Measurements of the redefined indices for spectral data examined here are given in Tables 6–12 (cols. [2]–[8]). In Figures 6 and 7 we plot the values of the H₂O and CH₄ indices as measured with the SpeX and CGS4 data, respectively, as a function of spectral type. All six ratios show monotonic decreases in value with later subtypes, with strong correlations. In particular, the H₂O-*H* index varies nearly linearly over the entire spectral type range. The H₂O-*J*, CH₄-*J*, and CH₄-*H* indices are slightly degenerate for the earliest T spectral types, while the CH₄-*K* index is degenerate between T7 and T8. The index H₂O-*K* shows the largest scatter as a function of spectral type, notably among late-type and peculiar sources. Indeed, for some data sets (e.g., OSIRIS), there is very poor correlation between this index and spectral type, likely due to increased noise caused by telluric absorption around the 1.9 μm H₂O band. We therefore omit this index from our classification set and focus on five primary classification indices: H₂O-*J*, CH₄-*J*, H₂O-*H*, CH₄-*H*, and CH₄-*K*.

4.2.2. Index Classification: Two Methods

The B02 and G02 schemes differ slightly in their use of spectral indices for classification. The former scheme directly compares measured indices to those of the standards, while the latter scheme specifies subtype ranges for each index. The B02 method is more closely aligned to the MK process in spirit, but the G02 method is a less cumbersome means of determining the classification of a particular T dwarf. As both of these techniques have been used in the literature, we examined them independently to determine whether any significant differences exist.

Index subtypes were first derived following the prescription of B02. Table 4 lists the spectral index values for the T dwarf

¹² These data, produced using the program IRTRANS4, were obtained from the UKIRT World Wide Web pages.

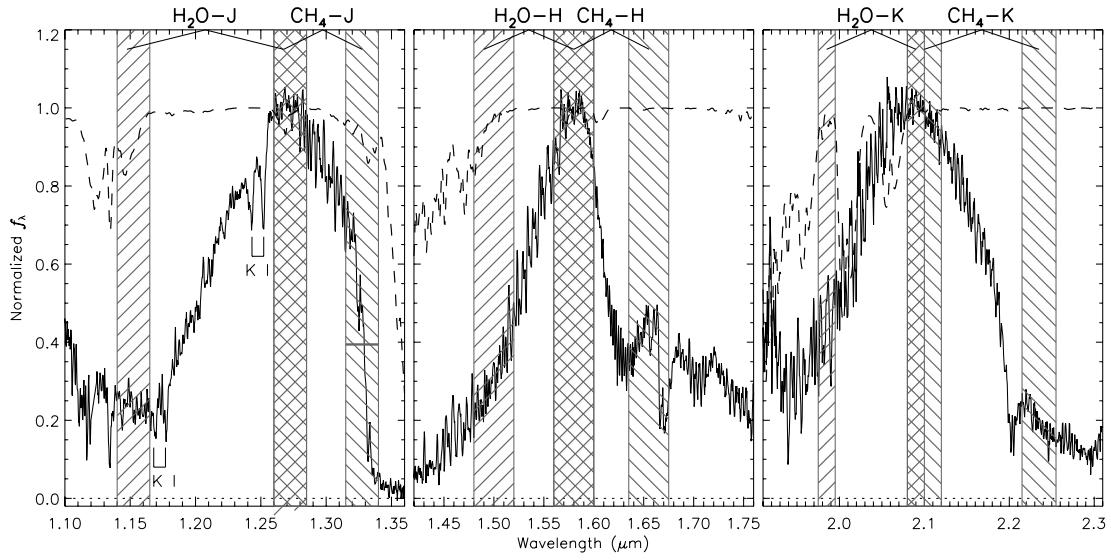


FIG. 5.—Spectral regions sampled by the six H₂O and CH₄ indices defined in Table 3, plotted on the NIR spectrum of the T5 standard 2MASS 1503+2525 (Burgasser et al. 2004). Not shown are the regions sampled by the K/J index. A telluric transmission spectrum typical for Mauna Kea is also shown (*dashed lines*) to highlight regions of low terrestrial atmospheric absorption. Spectral data in each panel are normalized at the local flux peak.

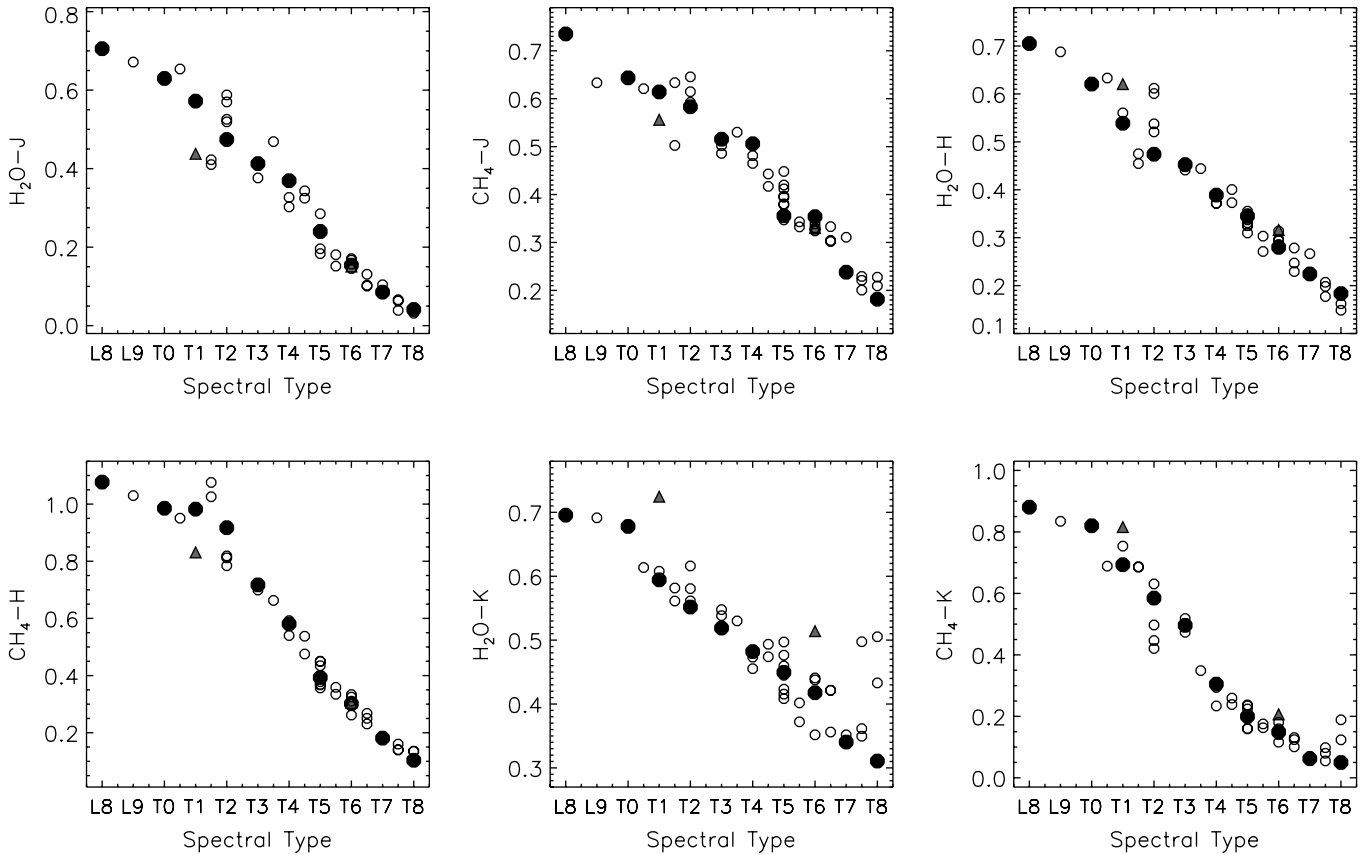


FIG. 6.—Values for the H₂O and CH₄ spectral indices measured on the SpeX prism data as a function of spectral type (as determined by direct spectral comparison). Primary standards are indicated by filled black circles, peculiar sources and uncertain classifications by filled gray triangles, and all other sources by open circles. Note the variable vertical scale in each panel.

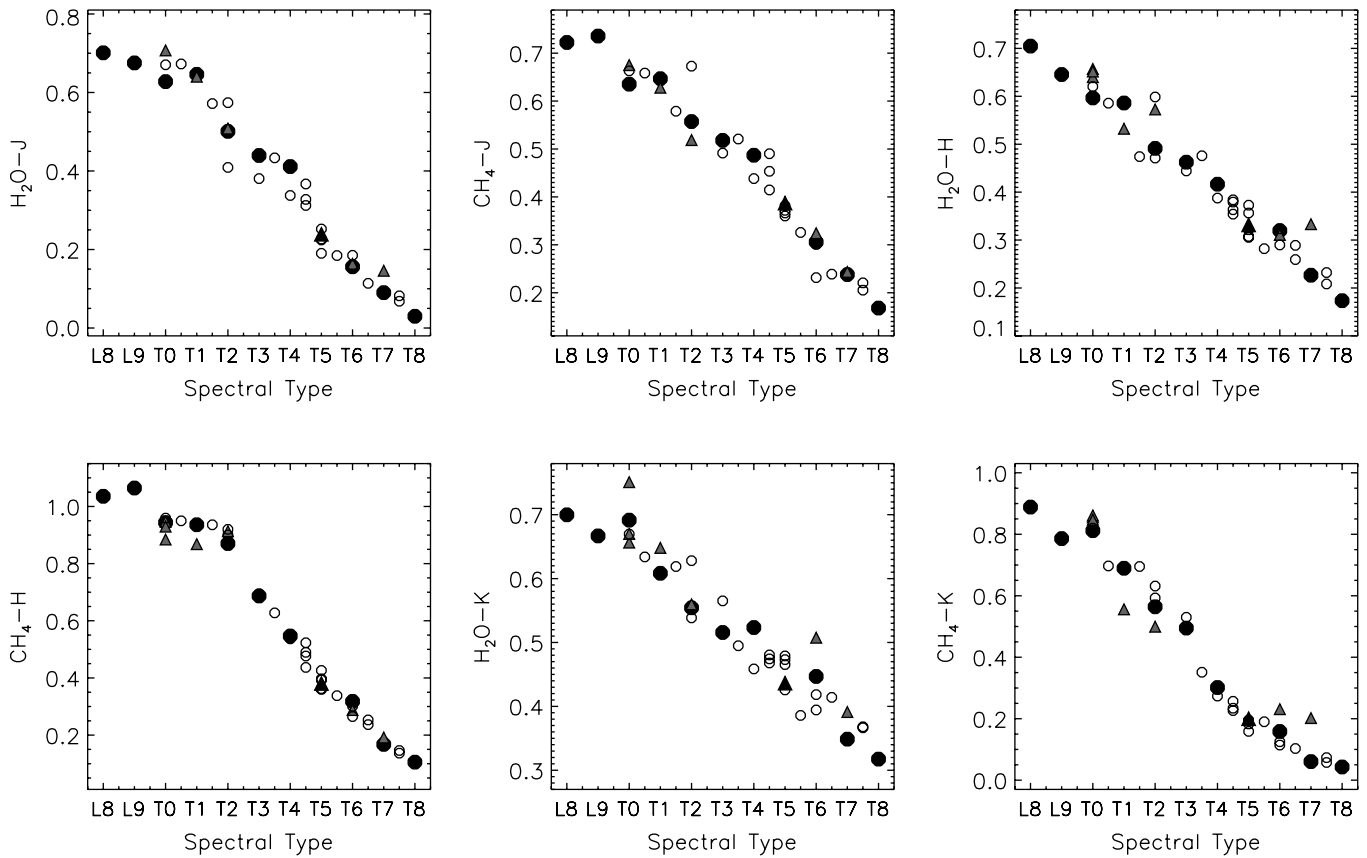


Fig. 7.—Same as Fig. 6, but for the CGS4 spectra.

TABLE 4
NEAR-INFRARED SPECTRAL INDICES FOR T DWARF SPECTRAL STANDARDS

Name (1)	NIR Spectral Type (2)	H ₂ O- <i>J</i> (3)	CH ₄ - <i>J</i> (4)	H ₂ O- <i>H</i> (5)	CH ₄ - <i>H</i> (6)	CH ₄ - <i>K</i> (7)
SpeX Prism Data						
2MASS 1632+1904	L8 ^a	0.706	0.735	0.705	1.077	0.881
SDSS 0423-0414 ^b	T0	0.630	0.644	0.621	0.985	0.820
SDSS 0837-0000	T1	0.572	0.614	0.539	0.982	0.693
SDSS 1254-0122	T2	0.474	0.583	0.474	0.917	0.585
2MASS 1209-1004	T3	0.413	0.516	0.453	0.717	0.496
2MASS 2254+3123	T4	0.369	0.506	0.389	0.581	0.305
2MASS 1503+2525	T5	0.240	0.356	0.345	0.393	0.200
SDSS 1624+0029	T6	0.154	0.354	0.280	0.301	0.149
2MASS 0727+1710	T7	0.085	0.238	0.224	0.181	0.062
2MASS 0415-0935	T8	0.041	0.182	0.183	0.104	0.050
CGS4 Data ^c						
2MASS 1632+1904	L8 ^a	0.701	0.722	0.705	1.036	0.888
2MASS 0310+1648	L9 ^a	0.675	0.736	0.645	1.064	0.786
SDSS 1207+0244	T0	0.628	0.635	0.597	0.944	0.812
SDSS 0837-0000	T1	0.646	0.647	0.586	0.936	0.689
SDSS 1254-0122	T2	0.501	0.557	0.491	0.870	0.564
2MASS 1209-1004	T3	0.439	0.518	0.462	0.687	0.495
2MASS 2254+3123	T4	0.411	0.487	0.416	0.547	0.302
2MASS 1503+2525	T5	0.239	0.387	0.332	0.381	0.200
SDSS 1624+0029	T6	0.156	0.306	0.320	0.318	0.158
2MASS 0727+1710	T7	0.090	0.238	0.227	0.168	0.060
2MASS 0415-0935	T8	0.030	0.168	0.173	0.105	0.043

^a Late L dwarf comparison source.

^b Alternate standard.

^c With the exception of SpeX cross-dispersed data for 2MASS 1503+2525 (Burgasser et al. 2004).

TABLE 5
 NUMERICAL RANGES OF NEAR-INFRARED SPECTRAL INDICES FOR T DWARF SUBTYPES

NIR Spectral Type (1)	H ₂ O- <i>J</i> (2)	CH ₄ - <i>J</i> (3)	H ₂ O- <i>H</i> (4)	CH ₄ - <i>H</i> (5)	CH ₄ - <i>K</i> (6)
T0.....	...	0.73–0.78	0.60–0.66	0.97–1.00	0.75–0.85
T1.....	>0.55	0.67–0.73	0.53–0.60	0.92–0.97	0.63–0.75
T2.....	0.45–0.55	0.58–0.67	0.46–0.53	0.80–0.92	0.55–0.63
T3.....	0.38–0.45	0.52–0.58	0.43–0.46	0.60–0.80	0.35–0.55
T4.....	0.32–0.38	0.45–0.52	0.37–0.43	0.48–0.60	0.24–0.35
T5.....	0.18–0.32	0.36–0.45	0.32–0.37	0.36–0.48	0.18–0.24
T6.....	0.13–0.18	0.28–0.36	0.26–0.32	0.25–0.36	0.13–0.18
T7.....	0.07–0.13	0.21–0.28	0.20–0.26	0.15–0.25	<0.13
T8.....	0.02–0.07	0.15–0.21	0.14–0.20	0.07–0.15	...

standards with SpeX and CGS4 data, in addition to values for the L8 and L9 comparison stars 2MASS 1632+1904 and 2MASS 0310+1648. As in B02, individual index subtypes were first determined as the closest match to the standard values (or half-subtype match). Subtypes for the CH₄-*H* index were only used for index values less than 1.0, as higher values are degenerate for L dwarfs and the earliest T dwarfs. Final classifications were determined as the average of the index subtypes; no rejection of outliers was made as in B02. Sources with a large scatter among the index subtypes (>1 subclass) or with only one spectral index measure available were noted as uncertain.

The second method, following the prescription of G02, involves the comparison of spectral indices to predefined ranges. Table 5 lists these ranges for the new indices, determined as the typical values for each spectral type as measured on the CGS4 data (i.e., Fig. 7). Because of their degeneracy, ranges for the H₂O-*J* and CH₄-*K* indices are only defined for spectral types \geq T2 and \leq T6, respectively. Index subtypes for each T dwarf were assigned according to the range the value falls in (or half-subtype for values close to range borders), and the average type was determined in the manner described above.

Tables 6–12 list the index-based spectral subtypes for the five primary classification ratios (cols. [2]–[6]), as well as the averaged types for all indices (cols. [10]–[11]). These classifications are generally equivalent to those determined by direct spectral comparison, as demonstrated in Figures 8 and 9 for the SpeX data set. Differences between the direct comparison and index-based classifications are generally less than 0.5–1 subtypes, with typical deviations of 0.3 subtypes. Hence, all three techniques yield results that are consistent within the nominal 0.5 subtype uncertainty of the scheme, and any could be used to classify the spectrum of a T dwarf. It is important to stress, however, that spectral indices are only proxies for the overall spectral morphology of a source, and direct spectral comparison to the standards is the most accurate and consistent means of classification (Morgan & Keenan 1973).

5. DISCUSSION

5.1. Revised Spectral Types and T Dwarf Properties

The revised classification scheme for T dwarfs presented here is similar in design to the schemes proposed by B02 and G02, in the choice of both spectral standards and spectral indices. Table 13 confirms this, comparing revised spectral types for 61 T dwarfs (based on direct spectral comparison) to prior classifications made on the B02 and G02 schemes. Nearly all of these are consistent within 0.5 subtypes; only seven differ by a full subclass (including the peculiar T7 Gl 229B; see below).

Hence, previously identified trends of absolute brightness (Dahn et al. 2002; Tinney et al. 2003; Vrba et al. 2004), color (B02; Leggett et al. 2002b; Knapp et al. 2004), and T_{eff} (Golimowski et al. 2004; Vrba et al. 2004) as a function of spectral type remain effectively unchanged.

Studies to date have demonstrated that for subtypes T5 and later, T spectral types are largely correlated with T_{eff} and luminosity (Golimowski et al. 2004; Vrba et al. 2004). This result is broadly consistent with the observed correlation between MK numerical type and temperature for main-sequence stars. However, the temperature correlation for earlier type T dwarfs is weak, with T_{eff} roughly constant from L8 to T5 despite significant changes in NIR spectral energy distributions (Kirkpatrick et al. 2000; B02; Dahn et al. 2002; Tinney et al. 2003; Golimowski et al. 2004; Nakajima et al. 2004; Vrba et al. 2004). The unusual properties of this spectral morphological transition, as well as the significant color variations found among similarly typed late-type T dwarfs (Knapp et al. 2004; Burgasser et al. 2005a), suggest that further extensions to the one-dimensional scheme defined here may be required. However, the clear variation in spectral morphologies of the standard stars across this transition implies that the scheme itself need not be redefined.

5.2. Extending the T Dwarf Spectral Sequence

5.2.1. Dust Effects in Early-Type T Dwarf Spectra

Condensate dust strongly influences the NIR spectra of L dwarfs and early-type T dwarfs but is largely absent in late-type T dwarf atmospheres (Tsuji et al. 1996; Allard et al. 2001). The depletion of dust from cool brown dwarf photospheres is now believed to play a greater role in the spectral transition between L and T dwarfs than T_{eff} (Ackerman & Marley 2001; B02; Tsuji & Nakajima 2003), although the mechanism for this depletion remains under considerable debate (Burgasser et al. 2002a; Knapp et al. 2004; Tsuji 2005). The composition and abundance of condensate dust species, as well as the thickness, density, and surface distribution of condensate cloud structures (Ackerman & Marley 2001), are likely to be complex functions of T_{eff} , surface gravity, metallicity, rotation, and other parameters (Helling et al. 2001, 2004; Lodders 2002; Woitke & Helling 2003, 2004); hence, substantial spectral variations among dust-dominated sources might be expected. Indeed, there appears to be a decoupling of optical and NIR spectral morphologies among late-type L dwarfs and early-type T dwarfs that could be indicative of such dust/ T_{eff} effects (Cruz et al. 2003; Knapp et al. 2004). A few of the early-type T dwarfs (e.g., 2MASS 0949–1545 and 2MASS 2139+0220; Tinney et al. 2005; K. L. Cruz et al. 2006,

TABLE 6
SPECTRAL INDICES AND CLASSIFICATIONS FOR SPeX PRISM SPECTRA

NAME (1)	H ₂ O- <i>J</i> (2)	CH ₄ - <i>J</i> (3)	H ₂ O- <i>H</i> (4)	CH ₄ - <i>H</i> (5)	CH ₄ - <i>K</i> (6)	H ₂ O- <i>K</i> (7)	<i>K</i> / <i>J</i> (8)	DERIVED NIR SPECTRAL TYPE		
								Direct (9)	Ind 1 (10)	Ind 2 (11)
2MASS 1632+1904	0.706 (L8.0/. . .)	0.735 (L8.0/T0.0)	0.705 (L8.0/. . .)	1.077 (. . ./ . .)	0.881 (L8.0/. . .)	0.696	0.743	L8.0	L8.0	. . .
DENIS 0255-4700	0.671 (L8.0/. . .)	0.633 (T0.5/T2.0)	0.688 (L8.0/. . .)	1.030 (. . ./ . .)	0.835 (T0.0/T0.0)	0.691	0.603	L9.0	L9.0:	. . .
SDSS 0423-0414.....	0.630 (T0.0/. . .)	0.644 (T0.0/T2.0)	0.621 (T0.0/T0.0)	0.985 (T0.0/T0.0)	0.820 (T0.0/T0.0)	0.678	0.477	T0.0	T0.0	T0.5:
SDSS 0151+1244	0.654 (L9.5/. . .)	0.621 (T1.0/T2.0)	0.633 (T0.0/T0.0)	0.951 (T1.5/T1.0)	0.689 (T1.0/T1.0)	0.614	0.429	T0.5	T0.5	T1.0
SDSS 0837-0000.....	0.573 (T1.0/. . .)	0.616 (T1.0/T2.0)	0.560 (T0.5/T1.0)	0.977 (T1.0/T0.5)	0.754 (T0.5/T0.5)	0.608	0.400	T1.0	T1.0	T1.0
	0.572 (T1.0/. . .)	0.614 (T1.0/T2.0)	0.539 (T1.0/T1.5)	0.982 (T1.0/T0.0)	0.693 (T1.0/T1.0)	0.594	0.411	T1.0	T1.0	T1.0
2MASS 2139+0220	0.423 (T3.0/T3.0)	0.503 (T4.0/T4.0)	0.475 (T2.0/T2.5)	1.026 (. . ./ . .)	0.685 (T1.0/T1.0)	0.582	0.408	T1.5	T2.5:	T2.5:
	0.410 (T3.0/T3.0)	0.634 (T0.5/T2.0)	0.455 (T3.0/T2.5)	1.076 (. . ./ . .)	0.687 (T1.0/T1.0)	0.561	0.392	T1.5	T2.0:	T2.0
2MASS 0518-2828	0.438 (T2.5/T2.5)	0.556 (T2.5/T3.0)	0.620 (T0.0/T0.0)	0.831 (T2.5/T2.0)	0.816 (T0.0/T0.0)	0.724	0.517	T1.0p	T1.5:	T1.5:
2MASS 0949-1545	0.588 (T0.5/. . .)	0.583 (T2.0/T2.5)	0.612 (T0.0/T0.5)	0.812 (T2.5/T2.5)	0.421 (T3.5/T3.0)	0.549	0.328	T2.0	T1.5:	T2.0:
	0.570 (T1.0/. . .)	0.615 (T1.0/T2.0)	0.601 (T0.0/T0.5)	0.819 (T2.5/T2.5)	0.447 (T3.5/T3.0)	0.581	0.341	T2.0	T1.5:	T2.0:
2MASS 1122-3512	0.526 (T1.5/T1.5)	0.592 (T1.5/T2.5)	0.521 (T1.5/T1.5)	0.784 (T2.5/T2.5)	0.497 (T3.0/T3.0)	0.561	0.287	T2.0	T2.0	T2.0
SDSS 1254-0122.....	0.474 (T2.0/T2.5)	0.583 (T2.0/T2.5)	0.474 (T2.0/T2.5)	0.917 (T2.0/T1.5)	0.585 (T2.0/T2.0)	0.552	0.365	T2.0	T2.0	T2.0
SDSS 1750+4222	0.519 (T1.5/T2.0)	0.646 (T0.0/T2.0)	0.538 (T1.0/T1.5)	0.913 (T2.0/T1.5)	0.631 (T1.5/T1.5)	0.616	0.369	T2.0	T1.0	T1.5
SDSS 1021-0304.....	0.376 (T4.0/T3.5)	0.486 (T4.0/T4.0)	0.448 (T3.0/T3.0)	0.712 (T3.0/T3.0)	0.518 (T3.0/T2.5)	0.538	0.289	T3.0	T3.5	T3.0
2MASS 1209-1004	0.408 (T3.0/T3.0)	0.502 (T4.0/T4.0)	0.441 (T3.0/T3.0)	0.699 (T3.0/T3.0)	0.473 (T3.0/T3.0)	0.548	0.274	T3.0	T3.0	T3.0
	0.413 (T3.0/T3.0)	0.516 (T3.0/T3.5)	0.453 (T3.0/T2.5)	0.717 (T3.0/T3.0)	0.496 (T3.0/T3.0)	0.519	0.264	T3.0	T3.0	T3.0
SDSS 1750+1759	0.469 (T2.0/T2.5)	0.530 (T3.0/T3.5)	0.444 (T3.0/T3.0)	0.663 (T3.5/T3.0)	0.349 (T4.0/T3.5)	0.530	0.226	T3.5	T3.0	T3.0
SDSS 0207+0000	0.303 (T4.5/T4.5)	0.481 (T4.0/T4.0)	0.372 (T4.5/T4.5)	0.540 (T4.0/T4.0)	0.234 (T4.5/T4.5)	0.455	0.232	T4.0	T4.5	T4.5
2MASS 2151-4853	0.327 (T4.5/T4.5)	0.465 (T4.5/T4.5)	0.372 (T4.5/T4.5)	0.592 (T4.0/T3.5)	0.294 (T4.0/T4.0)	0.473	0.196	T4.0	T4.5	T4.0
2MASS 2254+3123	0.369 (T4.0/T3.5)	0.506 (T4.0/T4.0)	0.389 (T4.0/T4.0)	0.581 (T4.0/T3.5)	0.305 (T4.0/T4.0)	0.482	0.239	T4.0	T4.0	T4.0
SDSS 0000+2554	0.325 (T4.5/T4.5)	0.417 (T4.5/T5.0)	0.373 (T4.5/T4.5)	0.538 (T4.0/T4.0)	0.259 (T4.5/T4.5)	0.474	0.198	T4.5	T4.5	T4.5
2MASS 0559-1404	0.343 (T4.0/T4.0)	0.443 (T4.5/T4.5)	0.400 (T4.0/T4.0)	0.476 (T4.5/T4.5)	0.239 (T4.5/T4.5)	0.494	0.188	T4.5	T4.5	T4.5
2MASS 0407+1514	0.236 (T5.0/T5.0)	0.397 (T4.5/T5.0)	0.341 (T5.0/T5.0)	0.367 (T5.5/T5.5)	0.161 (T6.0/T6.0)	0.423	0.205	T5.0	T5.0	T5.5
2MASS 0755+2212	0.238 (T5.0/T5.0)	0.379 (T5.0/T5.5)	0.350 (T5.0/T5.0)	0.378 (T5.0/T5.5)	0.224 (T5.0/T5.0)	0.476	0.155	T5.0	T5.0	T5.0
2MASS 1503+2525	0.240 (T5.0/T5.0)	0.356 (T5.0/T5.5)	0.345 (T5.0/T5.0)	0.393 (T5.0/T5.0)	0.200 (T5.0/T5.0)	0.450	0.151	T5.0	T5.0	T5.0
2MASS 1828-4849	0.183 (T5.5/T5.5)	0.347 (T6.0/T5.5)	0.310 (T5.5/T5.5)	0.369 (T5.5/T5.5)	0.197 (T5.0/T5.0)	0.459	0.170	T5.0	T5.5	T5.5
2MASS 1901+4718	0.285 (T4.5/T4.5)	0.420 (T4.5/T5.0)	0.355 (T5.0/T5.0)	0.435 (T5.0/T5.0)	0.237 (T4.5/T4.5)	0.497	0.171	T5.0	T4.5	T5.0
SDSS 2124+0059	0.245 (T5.0/T5.0)	0.448 (T4.5/T4.5)	0.337 (T5.0/T5.0)	0.399 (T5.0/T5.0)	0.193 (T5.0/T5.5)	0.415	0.191	T5.0	T5.0	T5.0
2MASS 2331-4718	0.196 (T5.5/T5.5)	0.394 (T4.5/T5.0)	0.325 (T5.5/T5.5)	0.450 (T4.5/T4.5)	0.205 (T5.0/T5.0)	0.445	0.205	T5.0	T5.0	T5.0
2MASS 2339+1352	0.243 (T5.0/T5.0)	0.380 (T5.0/T5.5)	0.325 (T5.5/T5.5)	0.449 (T4.5/T5.0)	0.234 (T4.5/T4.5)	0.448	0.163	T5.0	T5.0	T5.0
2MASS 2356-1553	0.237 (T5.0/T5.0)	0.412 (T4.5/T5.0)	0.331 (T5.0/T5.5)	0.357 (T5.5/T5.5)	0.159 (T6.0/T6.0)	0.408	0.197	T5.0	T5.0	T5.5
SDSS 1110+0116.....	0.152 (T6.0/T6.0)	0.333 (T6.0/T6.0)	0.303 (T5.5/T6.0)	0.335 (T5.5/T5.5)	0.175 (T5.5/T5.5)	0.402	0.217	T5.5	T5.5	T6.0
2MASS 1231+0847	0.181 (T5.5/T5.5)	0.343 (T6.0/T5.5)	0.271 (T6.0/T6.5)	0.359 (T5.5/T5.5)	0.163 (T5.5/T6.0)	0.372	0.157	T5.5	T5.5	T6.0
2MASS 0243-2453	0.145 (T6.0/T6.0)	0.324 (T6.5/T6.0)	0.297 (T5.5/T6.0)	0.334 (T5.5/T5.5)	0.160 (T6.0/T6.0)	0.438	0.197	T6.0	T6.0	T6.0
2MASS 0937+2931	0.151 (T6.0/T6.0)	0.330 (T6.0/T6.0)	0.316 (T5.5/T5.5)	0.305 (T6.0/T6.0)	0.206 (T5.0/T5.0)	0.514	0.076	T6.0p	T5.5	T5.5
2MASS 1225-2739	0.171 (T6.0/T5.5)	0.331 (T6.0/T6.0)	0.286 (T6.0/T6.0)	0.325 (T5.5/T6.0)	0.180 (T5.5/T5.5)	0.441	0.147	T6.0	T6.0	T6.0
SDSS 1624+0029	0.167 (T6.0/T6.0)	0.339 (T6.0/T6.0)	0.314 (T5.5/T5.5)	0.311 (T6.0/T6.0)	0.141 (T6.0/T6.5)	0.416	0.156	T6.0	T6.0	T6.0
	0.154 (T6.0/T6.0)	0.354 (T6.0/T5.5)	0.280 (T6.0/T6.0)	0.301 (T6.0/T6.0)	0.149 (T6.0/T6.0)	0.418	0.142	T6.0	T6.0	T6.0

TABLE 6—Continued

NAME (1)	H ₂ O- <i>J</i> (2)	CH ₄ - <i>J</i> (3)	H ₂ O- <i>H</i> (4)	CH ₄ - <i>H</i> (5)	CH ₄ - <i>K</i> (6)	H ₂ O- <i>K</i> (7)	<i>K/J</i> (8)	DERIVED NIR SPECTRAL TYPE		
								Direct (9)	Ind 1 (10)	Ind 2 (11)
2MASS 2228–4310	0.157 (T6.0/T6.0)	0.328 (T6.0/T6.0)	0.293 (T6.0/T6.0)	0.262 (T6.5/T6.5)	0.116 (T6.5/...)	0.352	0.204	T6.0	T6.0	T6.0
2MASS 0034+0523	0.103 (T6.5/T7.0)	0.333 (T6.0/T6.0)	0.229 (T7.0/T7.0)	0.231 (T6.5/T6.5)	0.131 (T6.0/T6.5)	0.421	0.100	T6.5	T6.5	T6.5
SDSS 1346–0031	0.131 (T6.5/T6.5)	0.304 (T6.5/T6.0)	0.278 (T6.0/T6.0)	0.268 (T6.5/T6.5)	0.124 (T6.5/...)	0.421	0.156	T6.5	T6.5	T6.5
SDSS 1758+4633	0.101 (T7.0/T7.0)	0.302 (T6.5/T6.0)	0.247 (T6.5/T6.5)	0.250 (T6.5/T6.5)	0.101 (T6.5/...)	0.356	0.200	T6.5	T6.5	T6.5
2MASS 0050–3322	0.104 (T6.5/T7.0)	0.311 (T6.5/T6.0)	0.266 (T6.0/T6.5)	0.184 (T7.0/T7.0)	0.070 (T7.0/...)	0.352	0.180	T7.0	T6.5	T6.5
2MASS 0727+1710	0.085 (T7.0/T7.0)	0.238 (T7.0/T7.0)	0.224 (T7.0/T7.0)	0.181 (T7.0/T7.0)	0.062 (T7.0/...)	0.340	0.164	T7.0	T7.0	T7.0
2MASS 1114–2618	0.039 (T8.0/T8.0)	0.201 (T8.0/T7.5)	0.177 (T8.0/T8.0)	0.160 (T7.5/T7.5)	0.080 (T7.0/...)	0.498	0.076	T7.5	T7.5	T8.0
2MASS 1217–0311	0.066 (T7.5/T7.5)	0.221 (T7.5/T7.5)	0.207 (T7.5/T7.5)	0.139 (T8.0/T7.5)	0.055 (T8.0/...)	0.361	0.179	T7.5	T7.5	T7.5
Gl 570D	0.063 (T8.0/T7.5)	0.229 (T7.0/T7.0)	0.198 (T8.0/T7.5)	0.141 (T8.0/T7.5)	0.098 (T6.5/...)	0.350	0.116	T7.5	T7.5	T7.5
2MASS 0939–2448	0.032 (T8.0/T8.0)	0.228 (T7.0/T7.0)	0.162 (T8.0/T8.0)	0.135 (T8.0/T7.5)	0.124 (T6.5/...)	0.505	0.063	T8.0	T7.5	T8.0
	0.038 (T8.0/T8.0)	0.209 (T8.0/T7.5)	0.149 (T8.0/T8.0)	0.135 (T8.0/T7.5)	0.189 (T5.0/T5.5)	0.433	0.059	T8.0	T7.5:	T7.5:
2MASS 0415–0935	0.041 (T8.0/T8.0)	0.182 (T8.0/T8.0)	0.183 (T8.0/T8.0)	0.104 (T8.0/T8.0)	0.050 (T8.0/...)	0.311	0.131	T8.0	T8.0	T8.0

NOTES.—Index subtypes in parentheses are determined by direct comparison to spectral standard ratios (Table 4) or spectral ratio ranges (Table 5); see § 4.2.2. Uncertain classifications are indicated by a colon; peculiar sources are indicated by “p.”

TABLE 7
SPECTRAL INDICES AND CLASSIFICATIONS FOR CGS4 SPECTRA

NAME (1)	H ₂ O- <i>J</i> (2)	CH ₄ - <i>J</i> (3)	H ₂ O- <i>H</i> (4)	CH ₄ - <i>H</i> (5)	CH ₄ - <i>K</i> (6)	H ₂ O- <i>K</i> (7)	<i>K</i> / <i>J</i> (8)	DERIVED NIR SPECTRAL TYPE		
								Direct (9)	Ind 1 (10)	Ind 2 (11)
2MASS 1632+1904.....	0.701 (L8.0/...)	0.722 (L8.0/T0.5)	0.705 (L8.0/...)	1.036 (.../...)	0.888 (L8.0/...)	0.700	0.769	L8.0	L8.0	...
2MASS 0310+1648.....	0.675 (L9.0/...)	0.736 (L9.0/T0.5)	0.645 (L9.0/T0.0)	1.064 (.../...)	0.786 (L9.0/T0.0)	0.667	0.683	L9.0	L9.0	...
SDSS 0423-0414.....	0.671 (L9.0/...)	0.663 (T1.0/T1.5)	0.620 (L9.5/T0.0)	0.959 (T0.0/T0.5)	0.820 (T0.0/T0.0)	0.670	0.493	T0.0	T0.0	T0.5
SDSS 1104+5548.....	0.657 (L9.0/L9.5)	0.947 (T0.0/T1.0)	0.855 (L8.0/...)	0.656	...	T0.0:	L9.0:	T0.5:
SDSS 1207+0244.....	0.628 (T0.0/...)	0.635 (T0.0/T2.0)	0.597 (T0.0/T0.5)	0.944 (T0.0/T1.0)	0.812 (T0.0/T0.0)	0.691	0.446	T0.0	T0.0	T1.0
SDSS 1516+0259.....	0.640 (L9.0/T0.0)	0.884 (T2.0/T2.0)	0.861 (L8.0/...)	0.751	...	T0.0:	L9.5:	T1.0:
SDSS 2047-0718.....	0.707 (L8.0/...)	0.675 (T1.0/T1.5)	0.652 (L9.0/L9.5)	0.930 (T1.0/T1.5)	0.847 (T0.0/L9.5)	0.670	0.514	T0.0:	T0.0:	T0.5:
SDSS 0151+1244.....	0.673 (L9.0/...)	0.658 (T1.0/T1.5)	0.586 (T1.0/T0.5)	0.950 (T0.0/T1.0)	0.697 (T1.0/T1.0)	0.634	0.421	T0.5	T0.5	T1.0
SDSS 0837-0000.....	0.646 (T1.0/...)	0.647 (T1.0/T2.0)	0.586 (T1.0/T0.5)	0.936 (T1.0/T1.0)	0.689 (T1.0/T1.0)	0.608	0.363	T1.0	T1.0	T1.0
SDSS 1632+4150.....	0.640 (T1.0/...)	0.628 (T0.0/T2.0)	0.532 (T1.5/T1.5)	0.868 (T2.0/T2.0)	0.556 (T2.0/T2.5)	0.648	0.330	T1.0:	T1.5	T2.0
SDSS 1157+0611.....	0.572 (T0.0/...)	0.579 (T2.0/T2.5)	0.474 (T2.5/T2.5)	0.936 (T1.0/T1.0)	0.695 (T1.0/T1.0)	0.619	0.420	T1.5	T1.5	T2.0
SDSS 0758+3247.....	0.409 (T4.0/T3.0)	0.557 (T2.0/T3.0)	0.471 (T2.5/T2.5)	0.900 (T1.5/T1.5)	0.632 (T1.5/T1.5)	0.539	0.359	T2.0	T2.5:	T2.5
SDSS 1254-0122.....	0.501 (T2.0/T2.0)	0.557 (T2.0/T3.0)	0.491 (T2.0/T2.0)	0.870 (T2.0/T2.0)	0.564 (T2.0/T2.5)	0.554	0.352	T2.0	T2.0	T2.5
SDSS 1521+0131.....	0.508 (T2.0/T2.0)	0.519 (T3.0/T3.5)	0.573 (T1.0/T1.0)	0.913 (T1.5/T1.5)	0.499 (T3.0/T3.0)	0.560	0.297	T2.0:	T2.0	T2.0:
SDSS 1750+4222.....	0.574 (T0.0/...)	0.673 (T1.0/T1.5)	0.599 (T0.0/T0.5)	0.920 (T1.0/T1.5)	0.593 (T2.0/T2.0)	0.628	0.342	T2.0	T1.0	T1.5
2MASS 1209-1004.....	0.439 (T3.0/T2.5)	0.518 (T3.0/T3.5)	0.462 (T3.0/T2.5)	0.687 (T3.0/T3.0)	0.495 (T3.0/T3.0)	0.516	0.253	T3.0	T3.0	T3.0
SDSS 1021-0304.....	0.381 (T4.0/T3.5)	0.491 (T4.0/T4.0)	0.444 (T3.5/T3.0)	0.694 (T3.0/T3.0)	0.530 (T2.5/T2.5)	0.565	0.291	T3.0	T3.5	T3.0
SDSS 1750+1759.....	0.433 (T3.0/T2.5)	0.521 (T3.0/T3.5)	0.476 (T2.5/T2.5)	0.628 (T3.5/T3.5)	0.351 (T3.5/T3.5)	0.495	0.226	T3.5	T3.0	T3.0
2MASS 2254+3123.....	0.411 (T4.0/T3.0)	0.487 (T4.0/T4.0)	0.416 (T4.0/T3.5)	0.547 (T4.0/T4.0)	0.302 (T4.0/T4.0)	0.523	0.202	T4.0	T4.0	T3.5
SDSS 0000+2554.....	0.338 (T4.5/T4.0)	0.438 (T4.5/T4.5)	0.388 (T4.5/T4.0)	0.537 (T4.0/T4.0)	0.274 (T4.5/T4.0)	0.459	0.197	T4.0	T4.5	T4.0
2MASS 0559-1404.....	0.328 (T4.5/T4.5)	0.453 (T4.5/T4.5)	0.384 (T4.5/T4.5)	0.477 (T4.5/T4.5)	0.234 (T4.5/T4.5)	0.474	0.179	T4.5	T4.5	T4.5
SDSS 0207+0000.....	0.312 (T4.5/T4.5)	0.490 (T4.0/T4.0)	0.379 (T4.5/T4.5)	0.523 (T4.0/T4.0)	0.226 (T4.5/T4.5)	0.480	0.214	T4.5	T4.5	T4.5
SDSS 0830+0128.....	0.354 (T4.5/T5.0)	0.437 (T4.5/T5.0)	T4.5	T4.5	T5.0
SDSS 0926+5847.....	0.367 (T4.5/T3.5)	0.415 (T4.5/T5.0)	0.363 (T4.5/T4.5)	0.490 (T4.5/T4.5)	0.257 (T4.5/T4.5)	0.468	0.206	T4.5	T4.5	T4.5
2MASS 2339+1352.....	0.227 (T5.0/T5.0)	0.372 (T5.0/T5.5)	0.305 (T6.0/T5.5)	0.426 (T4.5/T5.0)	0.196 (T5.0/T5.0)	0.465	0.148	T5.0	T5.0	T5.0
SDSS 0741+2351.....	0.224 (T5.0/T5.0)	0.367 (T5.5/T5.5)	0.308 (T6.0/T5.5)	0.360 (T5.5/T5.5)	0.183 (T5.5/T5.5)	0.426	0.156	T5.0	T5.5	T5.5
SDSS 0742+2055.....	0.252 (T5.0/T5.0)	0.382 (T5.0/T5.5)	0.356 (T4.5/T5.0)	0.363 (T5.5/T5.5)	0.193 (T5.0/T5.5)	0.473	0.136	T5.0	T5.0	T5.5
SDSS 1110+0116.....	0.190 (T5.5/T5.5)	0.360 (T5.5/T5.5)	0.321 (T6.0/T5.5)	0.397 (T5.0/T5.0)	0.159 (T6.0/T6.0)	0.479	0.232	T5.0	T5.5	T5.5
SDSS 2124+0059.....	0.373 (T4.5/T4.5)	0.392 (T5.0/T5.0)	T5.0	T5.0	T5.0
2MASS 1231+0847.....	0.185 (T5.5/T5.5)	0.326 (T6.0/T6.0)	0.282 (T6.5/T6.0)	0.338 (T5.5/T5.5)	0.190 (T5.0/T5.5)	0.386	0.156	T5.5	T5.5	T5.5
2MASS 0937+2931.....	0.164 (T6.0/T6.0)	0.324 (T6.0/T6.0)	0.311 (T6.0/T5.5)	0.288 (T6.0/T6.0)	0.231 (T4.5/T4.5)	0.507	0.068	T6.0p	T5.5	T5.5
2MASS 1225-2739.....	0.185 (T5.5/T5.5)	0.301 (T6.0/T6.0)	0.323 (T5.5/T5.5)	0.301 (T6.0/T6.0)	0.125 (T6.5/...)	0.394	0.147	T6.0	T6.0	T6.0
SDSS 1346-0031.....	0.159 (T6.0/T6.0)	0.232 (T7.0/T7.0)	0.290 (T6.5/T6.0)	0.265 (T6.5/T6.5)	0.114 (T6.5/...)	0.418	0.170	T6.0	T6.5	T6.5
SDSS 1624+0029.....	0.156 (T6.0/T6.0)	0.306 (T6.0/T6.0)	0.320 (T6.0/T5.5)	0.318 (T6.0/T6.0)	0.158 (T6.0/T6.0)	0.447	0.140	T6.0	T6.0	T6.0
2MASS 1047+2124.....	0.259 (T6.5/T6.5)	0.253 (T6.5/T6.5)	T6.5	T6.5	T6.5
SDSS 1758+4633.....	0.114 (T6.5/T7.0)	0.239 (T7.0/T7.0)	0.289 (T6.5/T6.0)	0.237 (T6.5/T6.5)	0.103 (T6.5/...)	0.414	0.160	T6.5	T6.5	T6.5
2MASS 0727+1707.....	0.090 (T7.0/T7.0)	0.238 (T7.0/T7.0)	0.227 (T7.0/T7.0)	0.168 (T7.0/T7.5)	0.060 (T7.0/...)	0.349	0.144	T7.0	T7.0	T7.0
GI 229B.....	0.146 (T6.0/T6.0)	0.243 (T7.0/T7.0)	0.333 (T5.0/T5.0)	0.192 (T7.0/T7.0)	0.202 (T5.0/T5.0)	0.391	0.135	T7.0p	T6.0:	T6.0:
2MASS 1217-0311.....	0.082 (T7.0/T7.5)	0.221 (T7.0/T7.5)	0.232 (T7.0/T7.0)	0.146 (T7.5/T7.5)	0.058 (T7.0/...)	0.366	0.164	T7.5	T7.0	T7.5
GI 570D.....	0.068 (T7.5/T7.5)	0.205 (T7.5/T7.5)	0.208 (T7.5/T7.5)	0.137 (T7.5/T7.5)	0.073 (T7.0/...)	0.368	0.105	T7.5	T7.5	T7.5
2MASS 0415-0935.....	0.030 (T8.0/T8.0)	0.168 (T8.0/T8.0)	0.173 (T8.0/T8.0)	0.105 (T8.0/T8.0)	0.043 (T8.0/...)	0.317	0.134	T8.0	T8.0	T8.0

NOTES.—Index subtypes in parentheses are determined by direct comparison to spectral standard ratios (Table 4) or spectral ratio ranges (Table 5); see § 4.2.2. Uncertain classifications are indicated by a colon; peculiar sources are indicated by “p.”

TABLE 8
SPECTRAL INDICES AND CLASSIFICATIONS FOR NIRC GRISM SPECTRA

NAME (1)	H ₂ O- <i>J</i> (2)	CH ₄ - <i>J</i> (3)	H ₂ O- <i>H</i> (4)	CH ₄ - <i>H</i> (5)	CH ₄ - <i>K</i> (6)	H ₂ O- <i>K</i> (7)	<i>K/J</i> (8)	DERIVED NIR SPECTRAL TYPE		
								Direct (9)	Ind 1 (10)	Ind 2 (11)
2MASS 0920+3517	0.761 (L8.0/...)	0.635 (T0.5/T2.0)	0.716 (L8.0/...)	0.964 (T1.5/T0.5)	0.860 (L8.0/...)	0.653	0.538	T0.0p	L9.0:	T1.5:
2MASS 2254+3123	0.453 (T2.5/T2.5)	0.366 (T5.0/T5.5)	0.425 (T3.5/T3.5)	0.558 (T4.0/T4.0)	0.266 (T4.5/T4.5)	0.549	0.191	T4.0	T4.0	T4.0:
2MASS 0559-1404	0.366 (T4.0/T3.5)	0.405 (T4.5/T5.0)	0.375 (T4.5/T4.5)	0.491 (T4.5/T4.5)	0.228 (T4.5/T4.5)	0.445	0.252	T4.5	T4.5	T4.5
	0.322 (T4.5/T4.5)	0.437 (T4.5/T4.5)	0.347 (T5.0/T5.0)	0.509 (T4.5/T4.5)	0.243 (T4.5/T4.5)	0.524	0.275	T4.5	T4.5	T4.5
2MASS 2339+1352	0.303 (T4.5/T4.5)	0.232 (T7.0/T7.0)	0.317 (T5.5/T5.5)	0.424 (T5.0/T5.0)	0.200 (T5.0/T5.0)	0.511	0.169	T5.0	T5.5	T5.5
2MASS 2356-1553	0.250 (T5.0/T5.0)	0.403 (T4.5/T5.0)	0.299 (T5.5/T6.0)	0.352 (T5.5/T5.5)	0.160 (T6.0/T6.0)	0.495	0.228	T5.5	T5.5	T5.5
2MASS 0243-2453	0.161 (T6.0/T6.0)	0.267 (T7.0/T6.5)	0.278 (T6.0/T6.0)	0.327 (T5.5/T6.0)	0.158 (T6.0/T6.0)	0.494	0.198	T6.0	T6.0	T6.0
2MASS 0937+2931	0.177 (T5.5/T5.5)	0.290 (T6.5/T6.5)	0.281 (T6.0/T6.0)	0.324 (T5.5/T6.0)	0.236 (T4.5/T4.5)	0.634	0.121	T6.0p	T5.5	T5.5
	0.181 (T5.5/T5.5)	0.282 (T6.5/T6.5)	0.314 (T5.5/T5.5)	0.296 (T6.0/T6.0)	0.214 (T5.0/T5.0)	0.577	0.097	T6.0p	T5.5	T5.5
S Ori 70	0.280 (T6.0/T6.0)	0.225 (T5.0/T4.5)	0.502	...	T6.0:	T5.5	T5.5:
2MASS 1047+2124	0.162 (T6.0/T6.0)	0.244 (T7.0/T7.0)	0.248 (T6.5/T6.5)	0.263 (T6.5/T6.5)	0.171 (T5.5/T5.5)	0.485	0.149	T6.5	T6.5	T6.5
	0.162 (T6.0/T6.0)	0.244 (T7.0/T7.0)	0.247 (T6.5/T6.5)	0.263 (T6.5/T6.5)	0.171 (T5.5/T5.5)	0.485	0.155	T6.5	T6.5	T6.5
2MASS 1237+6526	0.123 (T6.5/T6.5)	0.245 (T7.0/T7.0)	0.233 (T7.0/T7.0)	0.239 (T6.5/T6.5)	0.156 (T6.0/T6.0)	0.520	0.101	T6.5	T6.5	T6.5
SDSS 1346-0031	0.146 (T6.0/T6.0)	0.267 (T7.0/T6.5)	0.271 (T6.0/T6.5)	0.273 (T6.0/T6.5)	0.161 (T6.0/T6.0)	0.485	0.182	T6.5	T6.0	T6.5
2MASS 0727+1710	0.104 (T6.5/T7.0)	0.223 (T7.5/T7.5)	0.218 (T7.0/T7.0)	0.196 (T7.0/T7.0)	0.100 (T6.5/...)	0.385	0.147	T7.0	T7.0	T7.0
2MASS 1217-0311	0.085 (T7.0/T7.0)	0.177 (T8.0/T8.0)	0.229 (T7.0/T7.0)	0.154 (T7.5/T7.5)	0.096 (T6.5/...)	0.422	0.205	T7.0	T7.0	T7.5
2MASS 1553+1532	0.112 (T6.5/T7.0)	0.185 (T8.0/T8.0)	0.223 (T7.0/T7.0)	0.192 (T7.0/T7.0)	0.093 (T6.5/...)	0.435	0.194	T7.0	T7.0	T7.5
Gl 229B	0.176 (T8.0/T8.0)	0.380 (T4.0/T4.5)	0.239 (T6.5/T6.5)	0.197 (T5.0/T5.0)	...	0.126	T7.0p	T6.0:	T6.0:
Gl 570D	0.071 (T7.5/T7.5)	0.195 (T8.0/T8.0)	0.177 (T8.0/T8.0)	0.153 (T7.5/T7.5)	0.074 (T7.0/...)	0.421	0.161	T7.5	T7.5	T8.0
2MASS 0415-0935	0.061 (T8.0/T7.5)	0.177 (T8.0/T8.0)	0.157 (T8.0/T8.0)	0.117 (T8.0/T8.0)	0.098 (T6.5/...)	0.353	0.209	T8.0	T7.5	T8.0
	0.054 (T8.0/T8.0)	0.186 (T8.0/T8.0)	0.162 (T8.0/T8.0)	0.114 (T8.0/T8.0)	0.064 (T7.0/...)	0.370	0.167	T8.0	T8.0	T8.0

NOTES.—Index subtypes in parentheses are determined by direct comparison to spectral standard ratios (Table 4) or spectral ratio ranges (Table 5); see § 4.2.2. Uncertain classifications are indicated by a colon; peculiar sources are indicated by “p.”

TABLE 9
SPECTRAL INDICES AND CLASSIFICATIONS FOR SPEX CROSS-DISPersed SPECTRA

NAME (1)	H ₂ O- <i>J</i> (2)	CH ₄ - <i>J</i> (3)	H ₂ O- <i>H</i> (4)	CH ₄ - <i>H</i> (5)	CH ₄ - <i>K</i> (6)	H ₂ O- <i>K</i> (7)	<i>K/J</i>	DERIVED NIR SPECTRAL TYPE		
								Direct (9)	Ind 1 (10)	Ind 2 (11)
DENIS 0255–4700	0.695 (L8.0/. . .)	0.718 (L8.0/T0.5)	0.684 (L8.0/. . .)	1.007 (. . ./. . .)	0.848 (T0.0/T0.0)	0.686	0.603	L9.0	L8.5:	. . .
SDSS 1254–0122.....	0.501 (T2.0/T2.0)	0.582 (T1.5/T2.5)	0.494 (T2.0/T2.0)	0.880 (T2.0/T2.0)	0.576 (T2.0/T2.0)	0.567	0.327	T2.0	T2.0	T2.0
2MASS 0559–1404	0.342 (T4.5/T4.0)	0.454 (T4.5/T4.5)	0.388 (T4.5/T4.0)	0.472 (T4.5/T4.5)	0.239 (T4.5/T4.5)	0.468	0.192	T4.5	T4.5	T4.5
2MASS 1503+2525	0.239 (T5.0/T5.0)	0.387 (T5.0/T5.0)	0.332 (T5.0/T5.5)	0.381 (T5.0/T5.5)	0.200 (T5.0/T5.0)	0.436	0.151	T5.0	T5.0	T5.0
2MASS 1901+4718	0.305 (T4.5/T4.5)	0.444 (T4.5/T4.5)	0.354 (T4.5/T5.0)	0.437 (T4.5/T5.0)	0.261 (T4.5/T4.5)	0.504	0.172	T5.0	T4.5	T4.5
2MASS 2331–4718	0.235 (T5.0/T5.0)	0.377 (T5.0/T5.5)	0.332 (T5.0/T5.5)	0.424 (T4.5/T5.0)	0.225 (T5.0/T4.5)	0.522	0.208	T5.0	T5.0	T5.0
2MASS 1231+0847	0.194 (T5.5/T5.5)	0.353 (T5.5/T5.5)	0.278 (T6.5/T6.0)	0.347 (T5.5/T5.5)	0.161 (T6.0/T6.0)	0.401	0.156	T5.5	T6.0	T5.5
2MASS 1828–4849	0.175 (T6.0/T5.5)	0.347 (T5.5/T5.5)	0.310 (T6.0/T5.5)	0.360 (T5.5/T5.5)	0.197 (T5.0/T5.0)	0.515	0.166	T5.5	T5.5	T5.5
2MASS 0034+0523	0.106 (T7.0/T7.0)	0.266 (T6.5/T6.5)	0.242 (T7.0/T7.0)	0.217 (T6.5/T7.0)	0.153 (T6.0/T6.0)	0.457	0.100	T6.5	T6.5	T6.5

NOTES.—Index subtypes in parentheses are determined by direct comparison to spectral standard ratios (Table 4) or spectral ratio ranges (Table 5); see § 4.2.2. Uncertain classifications are indicated by a colon; peculiar sources are indicated by “p.”

TABLE 10
SPECTRAL INDICES AND CLASSIFICATIONS FOR NIRSPEC SPECTRA

NAME (1)	H ₂ O- <i>J</i> (2)	CH ₄ - <i>J</i> (3)	H ₂ O- <i>H</i> (4)	CH ₄ - <i>H</i> (5)	CH ₄ - <i>K</i> (6)	H ₂ O- <i>K</i> (7)	<i>K/J</i> (8)	DERIVED NIR SPECTRAL TYPE		
								Direct (9)	Ind 1 (10)	Ind 2 (11)
2MASS 1632+1904	0.649 (T1.0/...)	0.723 (L8.0/T0.5)	0.696 (L8.0/...)	1.042 (.../...)	0.892 (L8.0/...)	0.683	0.898	L8.0	L8.5:	...
2MASS 0310+1648	0.679 (T1.0/T1.5)	L9.0	T1.0:	T1.5:
GI 337CD.....	0.632 (T0.0/...)	0.712 (L8.0/T1.0)	0.697 (L8.0/...)	0.973 (T0.0/T0.5)	0.789 (L9.0/T0.0)	0.685	0.712	T0.0	L9.0:	T0.5
SDSS 0423-0414.....	0.605 (T0.0/...)	0.656 (T1.0/T1.5)	0.615 (L9.5/T0.0)	0.956 (T0.0/T1.0)	0.826 (T0.0/T0.0)	0.658	0.558	T0.0	T0.0	T0.5
SDSS 0151+1244	0.655 (T1.0/T1.5)	T1.0	T1.0:	T1.5:
SDSS 0837-0000.....	...	0.641 (T0.0/T2.0)	0.569 (T1.0/T1.0)	0.991 (L8.0/T0.0)	0.710 (T1.0/T1.0)	0.599	0.306	T1.0	T0.0:	T1.0
SDSS 1254-0122.....	0.465 (T2.5/T2.5)	0.554 (T2.0/T3.0)	0.474 (T2.5/T2.5)	0.886 (T2.0/T2.0)	0.573 (T2.0/T2.0)	0.548	0.294	T2.0	T2.0	T2.5
SDSS 1021-0304.....	...	0.503 (T3.5/T4.0)	T3.0	T3.5:	T4.0:
SDSS 1750+1759	0.541 (T2.5/T3.0)	T3.5	T2.5:	T3.0:
2MASS 2254+3123	0.330 (T4.5/T4.5)	0.476 (T4.0/T4.0)	0.403 (T4.0/T4.0)	0.551 (T4.0/T4.0)	0.264 (T4.5/T4.5)	0.500	0.167	T4.0	T4.0	T4.0
2MASS 0559-1404	0.320 (T4.5/T4.5)	0.458 (T4.5/T4.5)	0.384 (T4.5/T4.5)	0.474 (T4.5/T4.5)	0.233 (T4.5/T4.5)	0.465	0.218	T4.5	T4.5	T4.5
SDSS 0926+5847	0.428 (T4.5/T4.5)	T4.5	T4.5:	T4.5:
2MASS 2356-1553	0.194 (T5.5/T5.5)	0.413 (T4.5/T5.0)	0.364 (T4.5/T4.5)	0.333 (T6.0/T5.5)	0.168 (T6.0/T5.5)	0.424	0.137	T5.5	T5.5	T5.0
SDSS 1624+0029	0.318 (T6.0/T6.0)	T6.0	T6.0:	T6.0:
2MASS 0727+1710	0.236 (T7.0/T7.0)	T7.0	T7.0:	T7.0:
2MASS 1237+6526	0.129 (T6.5/T6.5)	0.265 (T6.5/T6.5)	T7.0	T6.5	T6.5
2MASS 1553+1532	0.244 (T7.0/T7.0)	T7.0	T7.0:	T7.0:
GI 570D	0.058 (T8.0/T7.5)	0.204 (T7.5/T7.5)	0.207 (T7.5/T7.5)	0.143 (T7.5/T7.5)	0.074 (T7.0/...)	0.353	0.081	T7.5	T7.5	T7.5
2MASS 0415-0935	0.038 (T8.0/T8.0)	0.171 (T8.0/T8.0)	...	0.119 (T8.0/T8.0)	0.090 (T6.5/...)	0.339	0.175	T8.0	T7.5	T8.0

NOTES.—Index subtypes in parentheses are determined by direct comparison to spectral standard ratios (Table 4) or spectral ratio ranges (Table 5); see § 4.2.2. Uncertain classifications are indicated by a colon; peculiar sources are indicated by “p.”

TABLE 11
SPECTRAL INDICES AND CLASSIFICATIONS FOR OSIRIS SPECTRA

NAME (1)	H ₂ O- <i>J</i> (2)	CH ₄ - <i>J</i> (3)	H ₂ O- <i>H</i> (4)	CH ₄ - <i>H</i> (5)	CH ₄ - <i>K</i> (6)	H ₂ O- <i>K</i> (7)	<i>K</i> / <i>J</i> (8)	DERIVED NIR SPECTRAL TYPE		
								Direct (9)	Ind 1 (10)	Ind 2 (11)
SDSS 0423–0414.....	...	0.628 (T0.0/T2.0)	0.615 (L9.5/T0.0)	0.923 (T1.0/T1.5)	0.822 (T0.0/T0.0)	0.687	0.470	T0.0	T0.0	T1.0:
SDSS 1254–0122.....	...	0.554 (T2.0/T3.0)	0.483 (T2.5/T2.0)	0.855 (T2.0/T2.0)	0.540 (T2.5/T2.5)	0.507	0.412	T2.0	T2.5	T2.5
2MASS 2254+3123.....	...	0.439 (T4.5/T4.5)	0.372 (T4.5/T4.5)	0.520 (T4.0/T4.0)	...	0.386	0.204	T4.0	T4.5	T4.5
2MASS 0559–1404.....	...	0.371 (T5.0/T5.5)	0.320 (T6.0/T5.5)	0.402 (T5.0/T5.0)	0.216 (T5.0/T5.0)	0.558	0.215	T4.5	T5.5	T5.5
2MASS 1534–2952.....	...	0.364 (T5.5/T5.5)	0.341 (T5.0/T5.0)	0.397 (T5.0/T5.0)	0.195 (T5.0/T5.0)	0.452	0.145	T5.0	T5.0	T5.0
2MASS 0243–2453.....	...	0.500 (T3.5/T4.0)	0.203 (T7.5/T7.5)	0.247 (T6.5/T6.5)	...	0.549	0.231	T6.0:	T6.0:	T6.0:
2MASS 0937+2931.....	...	0.311 (T6.0/T6.0)	0.268 (T6.5/T6.5)	0.261 (T6.5/T6.5)	0.089	T6.0p	T6.5	T6.5
2MASS 1225–2739.....	...	0.306 (T6.0/T6.0)	0.259 (T6.5/T6.5)	0.278 (T6.5/T6.0)	...	0.298	0.137	T6.0	T6.5	T6.0
2MASS 1546–3325.....	...	0.316 (T6.0/T6.0)	0.303 (T6.0/T6.0)	0.302 (T6.0/T6.0)	...	0.367	0.152	T6.0	T6.0	T6.0
2MASS 2228–4310.....	...	0.305 (T6.0/T6.0)	0.261 (T6.5/T6.5)	0.228 (T6.5/T6.5)	0.061 (T7.0/...)	0.337	0.149	T6.0	T6.5	T6.5
2MASS 2356–1553.....	...	0.333 (T5.5/T6.0)	0.309 (T6.0/T5.5)	0.272 (T6.5/T6.5)	...	0.398	0.182	T6.0	T6.0	T6.0
SDSS 1624+0029.....	...	0.277 (T6.5/T6.5)	0.150 (T8.0/T8.0)	0.175 (T7.0/T7.5)	...	0.319	0.102	T6.0	T7.0	T7.5:
2MASS 0243–2453.....	...	0.278 (T6.5/T6.5)	0.270 (T6.5/T6.5)	0.254 (T6.5/T6.5)	0.139 (T6.0/T6.5)	0.390	0.143	T6.0	T6.5	T6.5
2MASS 0516–0445.....	...	0.307 (T6.0/T6.0)	0.309 (T6.0/T5.5)	0.214 (T6.5/T7.0)	0.173 (T5.5/T5.5)	0.393	0.255	T6.0	T6.0	T6.0
2MASS 2228–4310.....	...	0.305 (T6.0/T6.0)	0.261 (T6.5/T6.5)	0.228 (T6.5/T6.5)	0.061 (T7.0/...)	0.337	0.149	T6.0	T6.5	T6.5
2MASS 0727+1710.....	...	0.331 (T5.5/T6.0)	0.214 (T7.0/T7.5)	0.138 (T7.5/T7.5)	0.142	T7.0	T6.5:	T7.0
2MASS 1553+1532.....	...	0.190 (T8.0/T8.0)	0.212 (T7.5/T7.5)	0.132 (T8.0/T7.5)	...	0.428	0.101	T7.0	T8.0	T7.5
2MASS 0348–6022.....	...	0.245 (T7.0/T7.0)	0.192 (T8.0/T7.5)	0.173 (T7.0/T7.5)	0.116 (T6.5/...)	0.282	0.205	T7.0	T7.0	T7.5
GI 570D.....	...	0.168 (T8.0/T8.0)	0.206 (T7.5/T7.5)	0.117 (T8.0/T8.0)	...	0.349	0.116	T7.5	T8.0	T8.0
2MASS 0415–0935.....	...	0.148 (T8.0/T8.0)	0.174 (T8.0/T8.0)	0.085 (T8.0/T8.0)	...	0.372	0.130	T8.0	T8.0	T8.0

NOTES.—Index subtypes in parentheses are determined by direct comparison to spectral standard ratios (Table 4) or spectral ratio ranges (Table 5); see § 4.2.2. Uncertain classifications are indicated by a colon; peculiar sources are indicated by “p.”

TABLE 12
SPECTRAL INDICES AND CLASSIFICATIONS FOR OTHER PUBLISHED SPECTRA

NAME (1)	H ₂ O- <i>J</i> (2)	CH ₄ - <i>J</i> (3)	H ₂ O- <i>H</i> (4)	CH ₄ - <i>H</i> (5)	CH ₄ - <i>K</i> (6)	H ₂ O- <i>K</i> (7)	<i>K/J</i> (8)	DERIVED NIR SPECTRAL TYPE			REFERENCES (12)
								Direct (9)	Ind 1 (10)	Ind 2 (11)	
2MASS 0920+3517	0.739 (L9.0/T0.5)	...	0.867 (T2.0/T2.0)	0.901 (L8.0/...)	0.657	0.610	T0.0p	L9.5:	T1.5:	1
ϵ Indi Ba	0.593 (T0.5/T0.5)	0.904 (T1.5/T1.5)	T1.0	T1.0	T1.0	2
SDSS 1254-0122.....	0.491 (T2.0/T2.0)	0.560 (T2.0/T3.0)	0.507 (T2.0/T2.0)	0.846 (T2.0/T2.0)	0.564 (T2.0/T2.5)	0.549	0.354	T2.0	T2.0	T2.5	3
IFA 0230-Z1.....	0.646 (T3.5/T3.5)	T3.0:	T3.5:	T3.5:	4
SDSS 1750+1759	0.471 (T2.5/T2.5)	0.507 (T3.5/T4.0)	0.475 (T2.5/T2.5)	0.605 (T3.5/T3.5)	0.416 (T3.5/T3.0)	0.602	0.176	T3.5	T3.0	T3.0	3
2MASS 0559-1404	0.333 (T4.5/T4.5)	0.451 (T4.5/T4.5)	0.426 (T4.0/T3.5)	0.490 (T4.5/T4.5)	0.256 (T4.5/T4.5)	0.627	0.173	T4.5	T4.5	T4.5	5
ϵ Indi Bb	0.345 (T5.0/T5.0)	0.306 (T6.0/T6.0)	T6.0	T5.5	T5.5	2
NT 1205-0744.....	0.112 (T6.5/T7.0)	0.326 (T6.0/T6.0)	0.140 (T8.0/T8.0)	0.244 (T6.5/T6.5)	0.240 (T4.5/T4.5)	0.376	0.159	T7.0	T6.5:	T6.5:	6
2MASS 1217-0311	0.067 (T7.5/T7.5)	0.201 (T8.0/T7.5)	0.223 (T7.0/T7.0)	0.129 (T8.0/T8.0)	0.092 (T6.5/...)	0.359	0.171	T7.5	T7.5	T7.5	3

NOTES.—Index subtypes in parentheses are determined by direct comparison to spectral standard ratios (Table 4) or spectral ratio ranges (Table 5); see § 4.2.2. Uncertain classifications are indicated by a colon; peculiar sources are indicated by “p.”

REFERENCES.—(1) Nakajima et al. 2001; (2) McCaughrean et al. 2004; (3) Nakajima et al. 2004; (4) Liu et al. 2002; (5) Burgasser et al. 2000b; (6) Cuby et al. 1999.

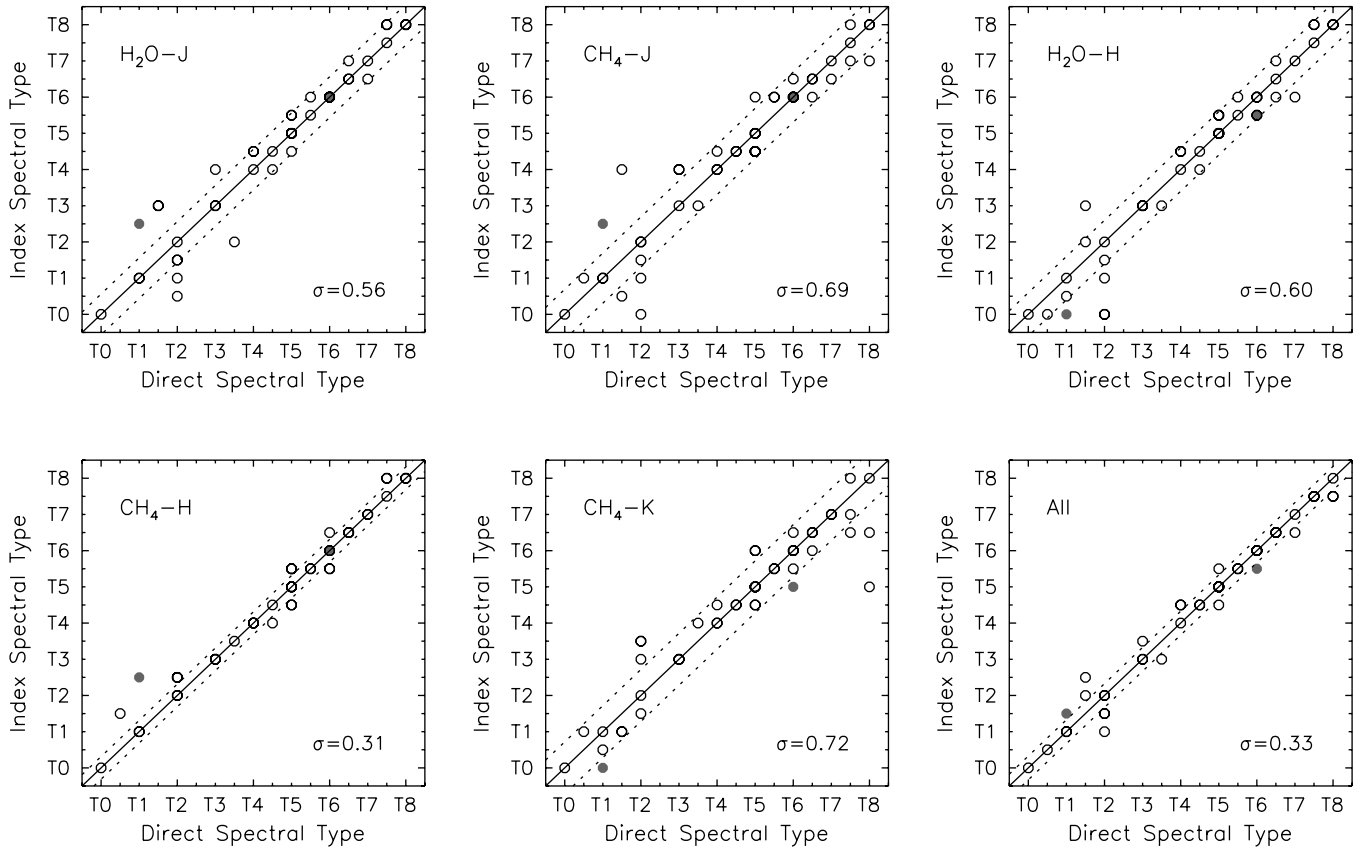


FIG. 8.—Comparison of index subtypes for the five primary classification indices, computed using the B02 method, vs. subtypes determined by direct spectral comparison for the SpeX prism data. Peculiar T dwarfs and uncertain classifications are indicated by filled gray circles, all others by open circles. The solid line delineates perfect agreement between subtypes, while the dotted lines indicate the $\pm 1 \sigma$ scatter in subtype deviations, as listed in each panel.

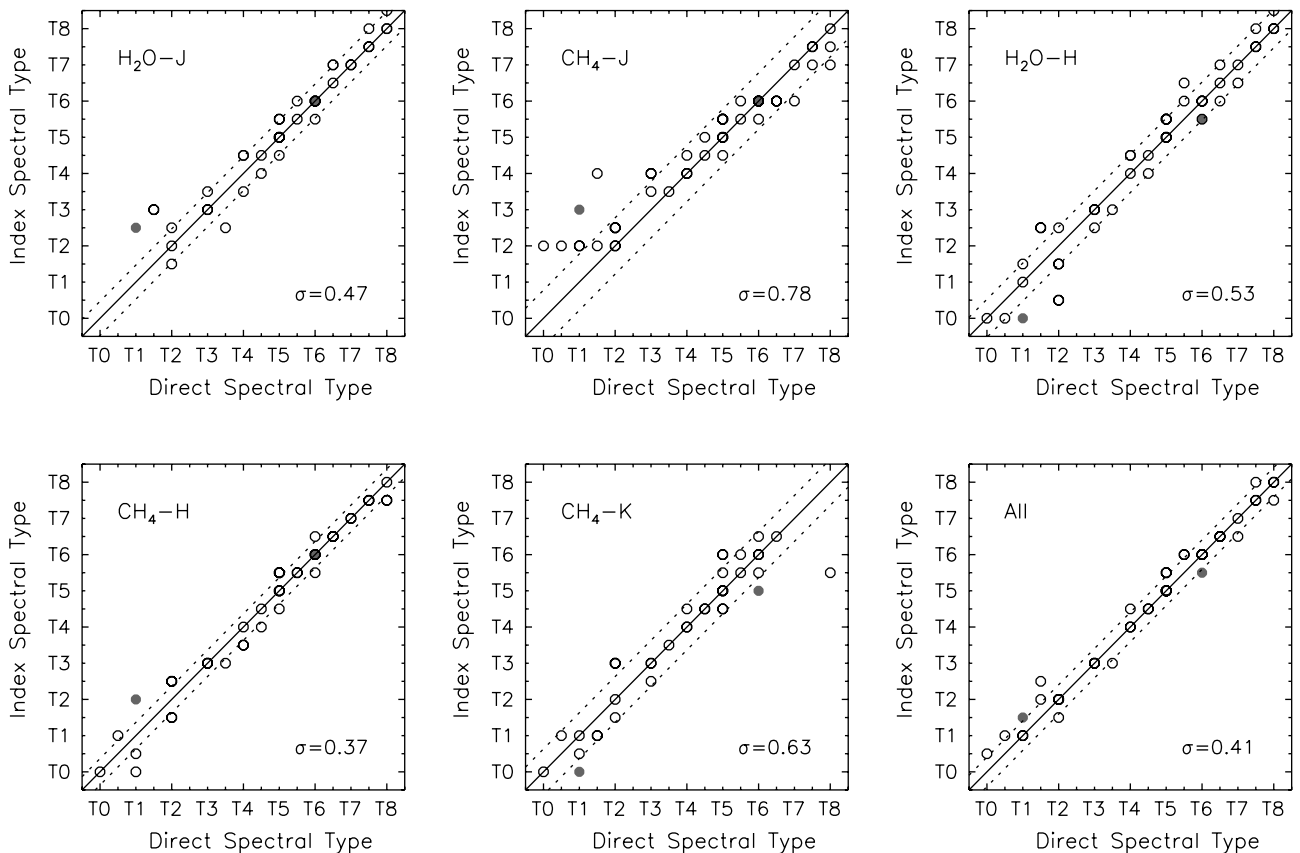


FIG. 9.—Same as Fig. 8, but comparing index subtypes computed using the G02 method. Note the absence of data points where the index ranges (Table 3) are not defined.

TABLE 13
COMPARISON OF T DWARF SPECTRAL TYPES

OBJECT (1)	NIR SPECTRAL TYPE		
	New (2)	B02 (3)	G02 (4)
SDSS 2047–0718.....	T0.0:	...	L9.5±1
SDSS 1104+5548.....	T0.0:	...	L9.5±1.5
SDSS 1207+0244.....	T0.0	...	T0
SDSS 1516+0259.....	T0.0:	...	T0±1.5
SDSS 0423–0414.....	T0.0	T0 ^a	T0
SDSS 0151+1244.....	T0.5	T0.5	T1±1
SDSS 0837–0000.....	T1.0	T1	T0.5
ϵ Indi Ba.....	T1.0	T1	T0.5
SDSS 1632+4150.....	T1.0:	...	T1±1
SDSS 1157+0611.....	T1.5	...	T1.5
2MASS 0949–1545.....	T2.0	T1 ^a	...
SDSS 1750+4222.....	T2.0	...	T1
2MASS 1122–3512.....	T2.0	T2 ^a	...
SDSS 0758+3247.....	T2.0	...	T2±1
SDSS 1521+0131.....	T2.0:	...	T2
SDSS 1254–0122.....	T2.0	T2	T2
2MASS 1209–1004.....	T3.0	T3 ^a	...
SDSS 1021–0304.....	T3.0	T3	T3
SDSS 1750+1759.....	T3.5	T3.5 ^a	T3.5
2MASS 2151–4853.....	T4.0	T4.5 ^a	...
2MASS 2254+3123.....	T4.0	T5	T4
SDSS 0000+2554.....	T4.5	...	T4.5
SDSS 0207+0000.....	T4.5	...	T4.5
SDSS 0926+5847.....	T4.5	...	T4.5
2MASS 0559–1404.....	T4.5	T5	T4.5
SDSS 0830+0128.....	T4.5	...	T5.5
2MASS 0755+2212.....	T5.0	T5:	...
2MASS 1901+4718.....	T5.0	T5 ^a	...
2MASS 2331–4718.....	T5.0	T5 ^a	...
SDSS 0742+2053.....	T5.0	...	T5
2MASS 0407+1514.....	T5.0	T5.5 ^a	...
2MASS 1503+2525.....	T5.0	T5.5	...
SDSS 0741+2351.....	T5.0	...	T5.5
2MASS 2339+1352.....	T5.0	T5.5	T5.5
2MASS 1828–4849.....	T5.0	T6 ^a	...
2MASS 2356–1553.....	T5.0	T6	...
SDSS 2124+0059.....	T5.0	...	T6
SDSS 1110+0116.....	T5.5	...	T5.5
2MASS 1231+0847.....	T5.5	T6 ^a	T5.5
ϵ Indi Bb.....	T6.0	T5.5	T5±1
2MASS 0516–0445.....	T6.0	T5.5	...
2MASS 0243–2453.....	T6.0	T6	...
2MASS 1225–2739.....	T6.0	T6	T6
SDSS 1624+0029.....	T6.0	T6	T6
2MASS 0937+2931.....	T6.0p	T6p	T6
2MASS 2228–4310.....	T6.0	T6.5	...
SDSS 1346–0031.....	T6.5	T6	T6
2MASS 1237+6526.....	T6.5	T6.5	...
2MASS 1047+2124.....	T6.5	T6.5	T6.5
2MASS 0034+0523.....	T6.5	T7	...
SDSS 1758+4633.....	T6.5	...	T7
NTTDF 1205–0744.....	T7.0:	T6:	...
Gl 229B.....	T7.0p	T6.5	T6±1
2MASS 0348–6022.....	T7.0	T7	...
2MASS 0727+1710.....	T7.0	T7	T8
2MASS 0050–3322.....	T7.0	T7.5 ^a	...
2MASS 1114–2618.....	T7.5	T7.5 ^a	...
2MASS 1217–0311.....	T7.5	T7.5	T8
Gl 570D.....	T7.5	T8	T8
2MASS 0939–2448.....	T8.0	T8 ^a	...
2MASS 0415–0935.....	T8.0	T8	T9

^a Based on revised indices similar to Table 3 (Burgasser et al. 2004; Tinney et al. 2005).

in preparation), while having overall spectral morphologies consistent with T1–T2 dwarfs, exhibit a much broader range of band strengths (and hence larger scatter in their index subtypes) and $J - K_s$ colors. While unresolved multiplicity cannot be ruled out for these sources (§ 6), the possible influence of dust-related spectral variations falls beyond the one-dimensional scheme defined here and may require an additional classification parameter.

The temporal evolution of dust-sensitive spectral features must also be characterized, particularly as this directly affects the stability of the spectral standards. While a number of studies have measured photometric variability of up to 0.5 mag in several L and T dwarfs (Bailer-Jones & Mundt 1999, 2001; Tinney & Tolley 1999; Gelino et al. 2002; Enoch et al. 2003; Bailer-Jones & Lamm 2003; Koen 2003, 2004), only one T dwarf has been monitored for spectral variations so far (SDSS 1624+0029; Nakajima et al. 2000). As the photometric variations have been linked to the surface evolution of condensate dust clouds (Gelino et al. 2002; Mohanty et al. 2002), verifying the spectral stability of the earliest type T standards, which are most affected by the photospheric condensates, should be a priority for future observational studies.

5.2.2. Gravity Effects in Late-Type T Dwarf Spectra

On the other end of the sequence, a handful of late-type T dwarfs, which exhibit otherwise normal band strengths, show significant variations in their K -band flux peaks as compared to the spectral standards. This phenomenon, cited extensively in the literature (B02; Burgasser et al. 2004, 2005a; Leggett et al. 2002b; Golimowski et al. 2004; Knapp et al. 2004), is caused by variations in collision-induced H_2 absorption, which is particularly strong in the atmospheres of the coldest brown dwarfs. Correlated variations are also seen in the strengths of the 1.25 μm K_1 lines (Knapp et al. 2004) and the 1.05 μm flux peak (Burgasser et al. 2005a). These spectral peculiarities are likely tied to differences in surface gravities and possibly metallicities among late-type T dwarfs (Saumon et al. 1994; Burrows et al. 2002; Burgasser et al. 2005a; Knapp et al. 2004) and can vary significantly for a given set of H_2O and CH_4 band strengths. This is demonstrated graphically in Figure 10, which compares the K/J and CH_4-H ratios for the SpeX prism data set.¹³ While the ratios show reasonable correlation over much of the T sequence, there is a substantial increase in the range of K/J values among the latest type T dwarfs. The decoupling of these “surface gravity features” from the standard classification sequence again suggests that a second classification parameter is required to fully describe the spectra.

While dust, gravity, and metallicity features may necessitate extensions to the one-dimensional scheme defined here, the inclusion of a second (or third or fourth) classification parameter under the MK process requires the identification of additional spectral standards to map out the new parameter space. As the number of “deviant” T dwarfs is still relatively small, we leave this task to a future study.

5.3. To the End of the T Dwarf Class and Beyond

The classification scheme defined here sufficiently encompasses the range of spectral morphologies observed for the known population of T dwarfs. But what about colder brown dwarfs

¹³ The SpeX data set is particularly useful for exploring this phenomenon as the entire 0.8–2.5 μm range is observed in a single dispersion order, mitigating flux scaling errors that can affect data obtained in multiple settings.

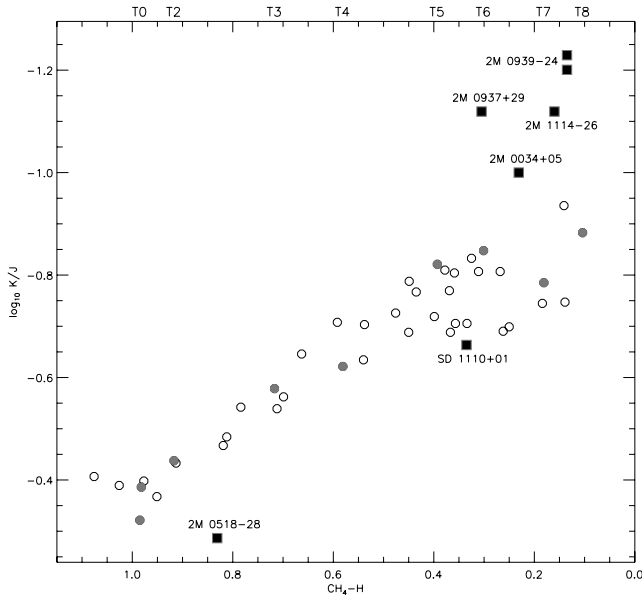


FIG. 10.—Comparison of K/J (on a logarithmic scale) and $\text{CH}_4\text{-}H$ indices as measured for SpeX prism data. Spectral standards are distinguished by gray circles. Sources suspected to have unusually high or low surface gravities or subsolar metallicities are indicated by black squares and labeled (2MASS 0518–2828 is separately discussed in § 6). The broad spread in the K/J indices among the late-type T dwarfs suggests that a second classification parameter may be required to fully describe their spectra.

that are likely to be identified in the near future? Assigning new T subtypes for such sources would require that they follow the same spectral trends as the latest type T dwarfs, namely, progressively stronger bands of H_2O and CH_4 . As these bands are already nearly saturated in the spectrum of the T8 standard 2MASS 0415–0935, it is unlikely that many more *readily distinguishable* T subtypes will be identified (Burrows et al. 2003). This is not to say that significantly cooler brown dwarfs could not be classified as late-type T dwarfs; these later subtypes may just encompass much broader T_{eff} intervals. Furthermore, there is no a priori reason that T subtypes could not extend to T10 and beyond, as is the case for the M giant sequence.

On the other hand, if the NIR spectral features of a cold brown dwarf discovery were significantly and systematically different than those examined here, a new spectral class, already referred to in the literature as the Y dwarf class (Kirkpatrick et al. 1999; Burrows et al. 2003; Knapp et al. 2004), would be required. How will these spectra differ? Theoretical atmosphere models predict several effects, including the emergence of NH_3 bands at 1.5 and 1.95 μm below $T_{\text{eff}} \sim 600$ K (the 10.5 μm band has already been detected in the spectrum of ϵ Indi Bab; Roellig et al. 2004); the disappearance of the strong pressure-broadened Na I and K I doublets, and weaker Cs I lines at 0.85 and 0.89 μm , below $T_{\text{eff}} \sim 500$ K; the condensation of H_2O vapor around 400–500 K; and the gradual transition to red NIR spectral energy distributions around 300–400 K (Burrows et al. 2003). Any of these NIR spectral transitions would signal a clear break between the T and Y spectral classes. Such a break could also arise at other wavelengths. Just as T dwarfs are distinguished from the (originally) optically classified L dwarfs by the presence of the NIR CH_4 bands (Kirkpatrick et al. 1999; G02), so too may Y dwarfs be distinguished by the emergence of distinct features longward of 2.5 μm , such as the 2.95 μm NH_3 band or broad H_2 features beyond 10 μm (Burrows et al. 2003). Until

examples of these cold brown dwarfs are actually identified, however, delineating the end of the T dwarf class is largely an exercise in speculation.

6. INDIVIDUAL SOURCES

A handful of sources studied here deserve additional attention, due to either their spectral peculiarity or significantly revised classification.

DENIS 0255–4700 (L9).—Identified by Martín et al. (1999) in the Deep Near Infrared Survey of the Southern Sky (DENIS; Epchtein et al. 1997), this relatively bright L dwarf (2MASS $J = 13.25 \pm 0.03$) is classified as L8 in the optical (J. D. Kirkpatrick et al. 2006, in preparation). Cushing et al. (2005) have detected weak CH_4 absorption at 1.6 and 2.2 μm in moderate-resolution SpeX data and suggest that this source could be classified as a T dwarf based on the definition put forth by G02. However, it is important to note that the analogous definition adopted here requires the detection of H -band CH_4 absorption at low spectral resolutions. Examination of SpeX prism data (A. J. Burgasser et al. 2006, in preparation; Fig. 11) reveals no distinct H -band CH_4 absorption feature (likely due to its weakness) and an overall spectral energy distribution consistent with a late-type L dwarf. Therefore, according to the scheme defined here, DENIS 0255–4700 is classified as $\sim\text{L9}$ in the NIR, of slightly earlier type than a T dwarf.

SDSS 1104+5548 and SDSS 2047–0718 (T0:).—Classified $\text{L}9.5 \pm 1.5$ and $\text{L}9.5 \pm 1.0$ by G02, respectively, these faint sources are reclassified as T0: based on their similarity to the T0 standard SDSS 1207+0244. Weak CH_4 absorption appears to be present at both 1.6 and 2.2 μm , although the low-S/N spectra of both sources make these assignments uncertain.

2MASS 0518–2828 (T1p).—The spectrum of this source is clearly peculiar (Fig. 3), with J - and H -band spectral features consistent with a subtype later than T2, but a K -band spectrum and red $J - K$ color consistent with a late-type L dwarf/early-type T dwarf. Cruz et al. (2004), who identified the source in the 2MASS database, have proposed that it is an unresolved binary composed of a mid/late-type L dwarf ($\sim\text{L6}$) and early/mid-type T dwarf ($\sim\text{T4}$). Confirmation of this hypothesis is forthcoming (K. L. Cruz 2005, private communication).

2MASS 0920+3517AB (T0p).—This source was identified by Kirkpatrick et al. (2000) in the 2MASS database and is classified as L6.5 in the optical. Spectroscopic observations by Nakajima et al. (2001) reveal the presence of CH_4 absorption at 1.6 and 2.2 μm , which are verified, but previously unrecognized, in low-resolution NIRC grism data (B02; Fig. 11). However, there are some spectral discrepancies; the 1.1 μm $\text{H}_2\text{O}/\text{CH}_4$ band is shallower than those observed in early-type T dwarfs, while the 2.2 μm CH_4 band is fairly weak compared to the 1.6 μm band. Like 2MASS 0518–2828, these features may arise from a composite spectrum of a late-type L dwarf and early-type T dwarf pair. 2MASS 0920+3517AB is marginally resolved as a closely separated ($\sim 0''.075$) binary in *HST* observations (Reid et al. 2001).¹⁴ Bouy et al. (2003) determine an F814W ($\lambda_c = 0.83 \mu\text{m}$) flux ratio of 0.88 ± 0.11 mag, implying $M_I \approx 19$ for 2MASS 0920+3517B, comparable to the I -band absolute magnitudes of late-type L dwarfs through mid-type T dwarfs (Dahn et al. 2002). A composite L/T spectrum might

¹⁴ Reid et al. (2001) also speculate that the 2MASS 0850–1057AB system, the L6 spectral standard on the Kirkpatrick et al. (1999) optical scheme, may harbor a T dwarf secondary.

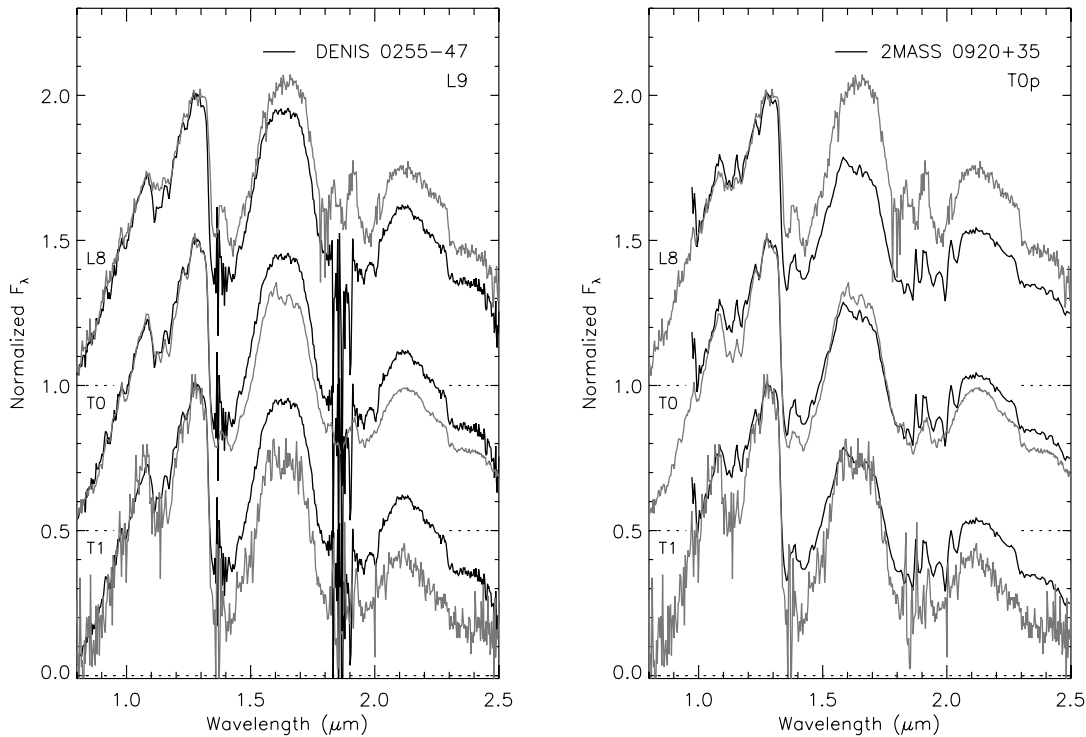


FIG. 11.—*Left*: Comparison of SpeX prism data for DENIS 0255–4700 (*black line*) to L8, T0, and T1 spectral standards (*gray lines*; note that the alternate standard SDSS 0423–0414AB is shown here). All of the spectra are normalized at their *J*-band flux peaks and offset by a constant (*dotted lines*). While Cushing et al. (2005) have detected CH₄ absorption at 1.6 μm in a higher resolution SpeX spectrum of DENIS 0255–4700, this band is not seen in these low-resolution data. *Right*: Similar comparison of NIRC grism data for 2MASS 0920+3517AB (B02). In this case CH₄ absorption at 1.6 μm is clearly present, although there are discrepancies in band strengths, e.g., the H₂O/CH₄ band at 1.1 μm as compared to the CH₄ band at 1.6 μm . This source is therefore classified as T0p in the NIR, much later than its L6.5 optical classification (Kirkpatrick et al. 2000).

also explain the large discrepancy between the optical spectral type and NIR spectral morphology of this source.

Gl 337CD (T0).—Identified by Wilson et al. (2001a) as a widely separated ($43'' \approx 880$ AU) common proper-motion companion to the G8 V+K1 V binary Gl 337AB, and itself resolved as a nearly equal brightness binary at *K* band (Burgasser et al. 2005b), this source is optically classified as L8 on the Kirkpatrick et al. (1999) scheme. Its NIR spectrum (McLean et al. 2003) exhibits distinct signatures of CH₄ absorption at both 1.6 and 2.2 μm that are similar to features in the T0 standard SDSS 1207+0244. The composite spectrum is therefore reclassified as T0 here. The small difference in absolute *K*-band magnitudes from L8 to T4 (Tinney et al. 2003; Golimowski et al. 2004; Vrba et al. 2004) suggests that this system could also be composed of a late-type L dwarf and early-type T dwarf pair.

2MASS 0937+2931 (T6p).—The prototype example of photospheric pressure effects in T dwarf spectra (§ 5.2.2), this peculiar T6 has been discussed extensively in the literature (B02; Burgasser et al. 2003b, 2005a; Golimowski et al. 2004; Knapp et al. 2004; Vrba et al. 2004). The current scheme retains the T6 classification of B02, but spectral peculiarities are clearly evident in both low-resolution (enhanced 1.05 μm peak, suppressed *K*-band peak) and moderate-resolution (weak 1.25 μm K 1 lines) data. 2MASS 0034+0523, 2MASS 0939–2448, and 2MASS 1114–2618 show similar, albeit less pronounced, spectral deviations (Burgasser et al. 2004, 2005a), while SDSS 1110+0116 exhibits enhanced *K*-band flux, suggesting that it is a low-gravity source (Knapp et al. 2004). The peculiar status of 2MASS 0937+2931 may therefore simply reflect the shortcomings of the one-dimensional classification scheme defined here.

Gl 229B (T7p).—One of the first brown dwarfs to be identified (Nakajima et al. 1995; Oppenheimer et al. 1995), this prototype T dwarf nevertheless fails to fit cleanly within the sequence of spectral standards. As shown in Figure 4, the CGS4 spectrum of Gl 229B (Geballe et al. 1996) exhibits strong CH₄ absorption at 1.3 and 1.6 μm , consistent with a T7 spectral type, but weaker H₂O and CH₄ bands at 1.1, 1.4, 1.9 and 2.2 μm , consistent with type T5–T6. Low-resolution NIRC grism data (Oppenheimer et al. 1998) show similar deviations. Because of its early discovery, there have been several detailed studies of Gl 229B suggesting that it may have atypical physical properties. Griffith et al. (1998) and Griffith & Yelle (2000) have proposed that the metallicity of Gl 229B may be 0.3–0.5 solar, based on spectral model fits to H₂O and Cs I features in its optical spectrum. Using spectral model fits for the M1 V primary, Leggett et al. (2002a) have also concluded that this system is metal-poor and possibly young as well. Both Gl 229B and 2MASS 0937+2931 are therefore important sources for studying the role of surface gravity and metallicity on the emergent spectra of the coldest known brown dwarfs.

7. SUMMARY

We have defined a revised NIR classification scheme for T dwarfs that unifies and supersedes original schemes proposed by B02 and G02. Nine primary spectral standards and five alternate standards define the scheme, and classifications for other sources may be made by the direct comparison of equivalent spectral data. Two alternate methods of classification using spectral indices have been described and shown to have no significant differences with direct spectral comparison. The

revised classifications are also consistent with the prior schemes, implying that existing analyses of spectral type trends remain intact. Nonetheless, we point out that future extensions to the one-dimensional classification scheme presented here may be needed to incorporate additional spectral variations. These extensions may be made when more examples of these objects are identified and characterized.

In the Appendix we provide a compendium of all T dwarfs with published NIR spectra at the time this article was written, listing classifications on the revised scheme. With 69 systems comprising this census, the study of cold brown dwarfs has crossed a threshold where detailed comparative analyses, population statistics, and the discovery and characterization of physically unique sources can be made. As forthcoming deep and wide-field sky surveys (e.g., UKIDSS; Warren 2002) uncover many more of our T dwarf neighbors, a unified framework for classifying these objects is clearly essential.

The authors give special thanks to K. Cruz, J. G. Cuby, M. Cushing, M. Liu, M. McCaughrean, I. S. McLean, T. Nakajima, B. Oppenheimer, R.-D. Scholz, and M. R. Zapatero Osorio for providing published and unpublished spectral data for this work and to K. Chiu and X. Fan for assistance with the retrieval of SDSS photometry. A. J. B. also thanks C. Corbally and R. Gray for useful insights on the MK process. We thank our anonymous referee for her/his helpful critique of the original manuscript. A. J. B. acknowledges support from NASA through the SIRTf Fellowship Program. T. R. G. acknowledges support by the Gemini Obser-

vatory, which is operated by the Association of Universities for Research in Astronomy, Inc., on behalf of the international Gemini partnership of Argentina, Australia, Brazil, Canada, Chile, the United Kingdom, and the United States of America. Some data were obtained through the UKIRT Service Programme. UKIRT is operated by the Joint Astronomy Centre on behalf of the UK Particle Physics and Astronomy Research Council. This publication makes use of data from the Two Micron All Sky Survey, which is a joint project of the University of Massachusetts and the Infrared Processing and Analysis Center and is funded by the National Aeronautics and Space Administration and the National Science Foundation. 2MASS data were obtained from the NASA/IPAC Infrared Science Archive, which is operated by the Jet Propulsion Laboratory, California Institute of Technology, under contract with the National Aeronautics and Space Administration. Funding for the Sloan Digital Sky Survey (SDSS) has been provided by the Alfred P. Sloan Foundation, the Participating Institutions, the National Aeronautics and Space Administration, the National Science Foundation, the US Department of Energy, the Japanese Monbukagakusho, and the Max-Planck Society. The SDSS Web site is <http://www.sdss.org>. The SDSS is managed by the Astrophysical Research Consortium (ARC) for the Participating Institutions. The Participating Institutions are the University of Chicago, Fermilab, the Institute for Advanced Study, the Japan Participation Group, Johns Hopkins University, the Korean Scientist Group, Los Alamos National Laboratory, the Max-Planck-Institute for Astronomy (MPIA), the Max-Planck-Institute for Astrophysics (MPA), New Mexico State University, University of Pittsburgh, University of Portsmouth, Princeton University, the United States Naval Observatory, and the University of Washington.

APPENDIX

T DWARF COMPENDIUM

Table 14 provides a compendium of all T dwarfs with published NIR spectra at the writing of this article and a sample of their empirical properties. This list includes 69 systems, including 9 binaries and 4 companions to main-sequence stars. NIR spectral types on the revised scheme are provided in column (2). Equinox J2000.0 coordinates, listed in columns (3) and (4), are primarily from the 2MASS All Sky Point Source Catalog (Cutri et al. 2003), with the exceptions of IFA 0226+0051, S Ori 70, SDSS 0837–0000, SDSS 1104+5548, SDSS 1157+0611, NTTDF 1205–0744, SDSS 1632+4150, and SDSS 2047–0718, for which positional data were obtained from the SDSS catalog or the discovery reference. Coordinate epochs are given in column (5). SDSS *z*-band magnitudes on the AB asinh system (Fukugita et al. 1996; Lupton et al. 1999) from the SDSS Data Release 4 (Adelman-McCarthy et al. 2006) are listed in column (6). 2MASS *JHK_s* photometry from the All Sky Catalog is listed in columns (7)–(9); for those sources undetected or marginally detected by 2MASS, alternate CIT or MKO¹⁵ *JHK* photometry is provided. Parallax (π ; col. [10]) and proper-motion (μ , ϕ ; cols. [11] and [12]) measurements from Dahn et al. (2002), Tinney et al. (2003), and Vrba et al. (2004) are listed for field sources and from *Hipparcos* (ESA 1997) for T dwarf companions to main-sequence stars. Additional proper-motion measurements from Burgasser et al. (2003c, 2003e, 2004), Ellis et al. (2005), and Tinney et al. (2005) are also listed. Relevant publications, including discovery citations, are provided in column (13). An electronic version of this table will be made available through the journal.

¹⁵ Note that photometry on the MKO system can be very different from photometry on the 2MASS or CIT systems. Values measured for T dwarfs in the former system can be found in Leggett et al. (2002b) and Knapp et al. (2004), and transformations between the MKO and 2MASS systems for late-type dwarfs are given in Stephens & Leggett (2004).

TABLE 14
T DWARF COMPENDIUM

NAME (1)	NIR SPECTRAL TYPE ^c (2)	J2000.0 COORDINATES ^a			SDSS ^d <i>z</i> (AB) (6)	2MASS ^b							REFERENCES ^c (13)
		α (3)	δ (4)	Epoch (5)		<i>J</i> (mag) (7)	<i>H</i> (mag) (8)	<i>K_s</i> (mag) (9)	π (mas) (10)	μ (arcsec yr ⁻¹) (11)	ϕ (deg) (12)		
SDSS J000013.54+255418.6.....	T4.5	00 00 13.54	+25 54 18 0	1998.76	18.48±0.04	15.06±0.04	14.73±0.07	14.84±0.12	1	
2MASS J00345157+0523050.....	T6.5	00 34 51.57	+05 23 05 0	2000.67	...	15.54±0.05	15.44±0.08	>16.2	...	0.68±0.06	72	2	
2MASS J00501994-3322402.....	T7	00 50 19.94	-33 22 40 2	1998.87	...	15.93±0.07	15.84±0.19	15.24±0.19	...	1.5±0.1	307	3	
SDSS J015141.69+124429.6.....	T1	01 51 41.55	+12 44 30 0	1997.70	19.40±0.07	16.57±0.13	15.60±0.11	15.18±0.19	47±3	0.743±0.004	93	4, 24	
SDSS J020742.48+000056.2.....	T4.5	02 07 42.84	+00 00 56 4	2000.63	20.08±0.12	16.63±0.05 ^f	16.66±0.05 ^f	16.62±0.05 ^f	35±10	0.156±0.011	96	4, 24, 25	
IFA 0230-Z1.....	T3	02 26 37.60	+00 51 54 7	2000.81	...	18.17±0.03 ^g	17.83±0.04 ^g	5	
2MASS J02431371-2453298.....	T6	02 43 13.71	-24 53 29 8	1998.86	...	15.38±0.05	15.14±0.11	15.22±0.17	94±4	0.355±0.004	234	6, 24	
2MASS J03480772-6022270.....	T7	03 48 07.72	-60 22 27 0	1999.88	...	15.32±0.05	15.56±0.14	15.60±0.23	...	0.77±0.04	201	7	
2MASS J04070885+1514565.....	T5	04 07 08.85	+15 14 56 5	1999.90	...	16.06±0.09	16.02±0.21	15.92±0.26	2	
2MASS J04151954-0935066.....	T8	04 15 19.54	-09 35 06 6	1998.87	...	15.70±0.06	15.54±0.11	15.43±0.20	174±3	2.255±0.003	76	6, 24	
SDSS J042348.57-041403.5AB.....	T0	04 23 48.58	-04 14 03 5	1998.73	17.33±0.03	14.47±0.03	13.46±0.04	12.93±0.03	65.9±1.7	0.333±0.003	284	4, 24, 27	
2MASS J05160945-0445499.....	T5.5	05 16 09.45	-04 45 49 9	1998.72	...	15.98±0.08	15.72±0.17	15.49±0.20	...	0.34±0.03	232	7	
2MASS J05185995-2828372.....	T1p	05 18 59.95	-28 28 37 2	1999.01	...	15.98±0.10	14.83±0.07	14.16±0.07	8	
S Ori 70.....	T6:	05 38 10.1	-02 36 26''	2000.85	...	20.28±0.10 ^h	20.42±0.11 ^h	19.78±0.17 ^h	9, 28	
2MASS J05591914-1404488.....	T4.5	05 59 19.14	-14 04 48 8	1998.95	...	13.80±0.02	13.68±0.04	13.58±0.05	97.7±1.3	0.6612±0.0012	122	10, 29	
Gl 229B.....	T7p	06 10 34.74 ⁱ	-21 51 59 5 ⁱ	1999.03	...	14.32±0.05 ^j	14.35±0.05 ^j	14.42±0.05 ^j	173.2±1.1	0.727±0.005	191	11, 26, 30, 31	
2MASS J07271824+1710012.....	T7	07 27 18.24	+17 10 01 2	1997.83	...	15.60±0.06	15.76±0.17	15.56±0.19	110±2	1.297±0.005	126	6, 24	
SDSS J074149.15+235127.5.....	T5	07 41 49.20	+23 51 27 5	1997.92	19.47±0.08	16.16±0.10	15.84±0.19	>15.9	1	
SDSS J074201.41+205520.5.....	T5	07 42 01.30	+20 55 19 8	1997.92	19.47±0.09	16.19±0.09	15.91±0.18	>15.2	1	
2MASS J07554795+2212169.....	T5	07 55 47.95	+22 12 16 9	1998.82	...	15.73±0.06	15.67±0.15	15.75±0.21	6	
SDSS J075840.33+324723.4.....	T2	07 58 40.37	+32 47 24 5	1998.34	17.97±0.02	14.95±0.04	14.11±0.04	13.88±0.06	1	
SDSS J083048.80+012831.1.....	T4.5	08 30 48.78	+01 28 31 1	2000.08	19.59±0.08	16.29±0.11	16.14±0.21	>16.4	1	
SDSS J083717.22-000018.3.....	T1	08 37 17.21	-00 00 18 0	1999.22	19.83±0.10	16.90±0.05 ^f	16.21±0.05 ^f	16.98±0.05 ^f	34±14	0.173±0.017	185	12, 24	
Gl 377CD.....	T0	09 12 14.69	+14 59 39 6	1997.88	...	15.51±0.08	14.62±0.08	14.04±0.06	48.8±0.9	0.5789±0.0014	295	13, 26, 32, 33	
2MASS J09201223+3517429AB.....	T0p	09 20 12.23	+35 17 42 9	1998.23	18.27±0.04	15.63±0.06	14.67±0.06	13.98±0.06	14, 35	
SDSS J092615.38+584720.9AB.....	T4.5	09 26 15.37	+58 47 21 2	2000.22	19.03±0.06	15.90±0.07	15.31±0.10	15.45±0.19	...	<0.3	...	4, 19, 36	
2MASS J09373487+2931409.....	T6p	09 37 34.87	+29 31 40 9	2000.25	...	14.65±0.04	14.70±0.07	15.27±0.13	163±4	1.622±0.007	143	6, 24	
2MASS J09393548-2448279.....	T8	09 39 35.48	-24 48 27 9	2000.11	...	15.98±0.11	15.80±0.15	>16.6	...	1.15±0.06	155	3	
2MASS J09490860-1545485.....	T2	09 49 08.60	-15 45 48 5	2000.19	...	16.15±0.12	15.26±0.11	15.23±0.17	...	0.10±0.04	271	3	
SDSS J102109.69-030420.1AB.....	T3	10 21 09.69	-03 04 19 7	1998.93	19.28±0.05	16.25±0.09	15.35±0.10	15.13±0.17	34±5	0.183±0.003	249	12, 36, 37	
2MASS J10475385+2124234.....	T6.5	10 47 53.85	+21 24 23 4	1998.08	...	15.82±0.06	15.80±0.12	>16.4	95±4	1.728±0.008	254	15, 24	
SDSS J110454.24+554841.3.....	T0:	11 04 54.25	+55 48 41 4	2001.89	19.94±0.10	17.31±0.05 ^f	16.71±0.05 ^f	16.31±0.05 ^f	1	
SDSS J111010.01+011613.1.....	T5.5	11 10 10.01	+01 16 13 0	2000.12	19.68±0.11	16.34±0.12	15.92±0.14	>15.1	...	0.34±0.10	110	4, 1, 3	
2MASS J11145133-2618235.....	T7.5	11 14 51.33	-26 18 23 5	1999.19	...	15.86±0.08	15.73±0.12	>16.1	...	3.05±0.04	263	3	
2MASS J11220826-3512363.....	T2	11 22 08.26	-35 12 36 3	1999.23	...	15.02±0.04	14.36±0.05	14.38±0.07	...	0.29±0.03	211	3	
SDSS J115700.50+061105.2.....	T1.5	11 57 00.50	+06 11 05 2	2001.14	20.21±0.11	17.09±0.05 ^f	16.45±0.05 ^f	16.00±0.05 ^f	1	
NTTDF 1205-0744.....	T6:	12 05 20.21	-07 44 01 0	1997.16	...	20.15 ^k	...	20.30 ^k	16	
SDSS J120747.17+024424.8.....	T0	12 07 47.17	+02 44 24 9	2000.13	18.39±0.04	15.58±0.07	14.56±0.07	13.99±0.06	...	0.39±0.09	286	1, 3	
2MASS J12095613-1004008.....	T3	12 09 56.13	-10 04 00 8	1999.10	...	15.91±0.07	15.33±0.09	15.06±0.14	...	0.46±0.10	140	2	
2MASS J12171110-0311131.....	T7.5	12 17 11.10	-03 11 13 1	1999.08	19.36±0.07	15.86±0.06	15.75±0.12	>15.9	91±2	1.0571±0.0017	274	15, 37	
2MASS J12255432-2739466AB.....	T6	12 25 54.32	-27 39 46 6	1998.51	...	15.26±0.05	15.10±0.08	15.07±0.15	75±3	0.737±0.003	149	15, 37, 38	
2MASS J12314753+0847331.....	T5.5	12 31 47.53	+08 47 33 1	2000.21	18.94±0.04	15.57±0.07	15.31±0.11	15.22±0.20	...	1.61±0.07	227	1, 2, 1 3	
2MASS J12373919+6526148.....	T6.5	12 37 39.19	+65 26 14 8	1999.20	19.56±0.08	16.05±0.09	15.74±0.15	>16.1	96±5	1.131±0.009	242	15, 24	
SDSS J125453.90-012247.4.....	T2	12 54 53.93	-01 22 47 4	1999.06	18.00±0.03	14.89±0.04	14.09±0.03	13.84±0.05	73.2±1.9	0.491±0.003	285	12, 37	

TABLE 14—Continued

NAME (1)	NIR SPECTRAL TYPE ^c (2)	J2000.0 COORDINATES ^a			SDSS ^d <i>z</i> (AB) (6)	2MASS ^b			π (mas) (10)	μ (arcsec yr ⁻¹) (11)	ϕ (deg) (12)	REFERENCES ^e (13)
		α (3)	δ (4)	Epoch (5)		<i>J</i> (mag) (7)	<i>H</i> (mag) (8)	<i>K_s</i> (mag) (9)				
SDSS J134646.45−003150.4	T6.5	13 46 46.34	−00 31 50 1	2001.09	19.16±0.05	16.00±0.10	15.46±0.12	15.77±0.27	68±2	0.516±0.003	257	17, 37
GI 570D	T7.5	14 57 14.96	−21 21 47 7	1998.37	...	15.32±0.05	15.27±0.09	15.24±0.16	169.3±1.7	2.012±0.004	149	18, 26
2MASS J15031961+2525196.....	T5	15 03 19.61	+25 25 19 6	1999.39	17.292±0.014	13.94±0.02	13.86±0.03	13.96±0.06	19
SDSS J151603.03+025928.9.....	T0:	15 16 03.03	+02 59 29 2	2000.31	19.60±0.08	17.23±0.20	16.00±0.15	15.43±0.18	1
SDSS J152103.24+013142.7.....	T2:	15 21 03.27	+01 31 42 6	2000.31	19.57±0.06	16.40±0.10	15.58±0.10	15.35±0.17	1
2MASS J15344984−2952274AB....	T5.5	15 34 49.84	−29 52 27 4	1998.52	...	14.90±0.05	14.87±0.10	14.84±0.11	73.6±1.2	0.2688±0.0019	159	6, 37, 38
2MASS J15462718−3325111.....	T5.5	15 46 27.18	−33 25 11 1	1998.52	...	15.63±0.05	15.45±0.09	15.49±0.18	88.0±1.9	0.225±0.002	33	6, 37
2MASS J15530228+1532369AB....	T7	15 53 02.28	+15 32 36 9	1998.14	...	15.83±0.07	15.94±0.16	15.51±0.18	6, 36
SDSS J162414.37+002915.6.....	T6	16 24 14.36	+00 29 15 8	1999.31	19.05±0.04	15.49±0.05	15.52±0.10	>15.5	92±2	0.3832±0.0019	270	20, 29
SDSS J163239.34+415004.3.....	T1:	16 32 39.34	+41 50 04 3	2001.39	20.35±0.11	16.87±0.05 ^f	16.42±0.05 ^f	16.19±0.05 ^f	1
SDSS J175024.01+422237.8.....	T2	17 50 23.85	+42 22 37 3	1998.44	19.38±0.09	16.47±0.10	15.42±0.09	15.48±0.17	1
SDSS J175032.96+175903.9.....	T3.5	17 50 32.93	+17 59 04 2	1999.23	19.63±0.06	16.34±0.10	15.95±0.13	15.48±0.19	36±5	0.204±0.008	61	4, 24
SDSS J175805.46+463311.9.....	T6.5	17 58 05.45	+46 33 09 9	1998.44	19.67±0.07	16.15±0.09	16.25±0.22	15.47±0.19	1
2MASS J18283572−4849046.....	T5.5	18 28 35.72	−48 49 04 6	2000.77	...	15.18±0.06	14.91±0.07	15.18±0.14	...	0.34±0.06	84	2, 3
2MASS J19010601+4718136.....	T5	19 01 06.01	+47 18 13 6	1998.47	...	15.86±0.07	15.47±0.09	15.64±0.29	...	0.38±0.22	17	2
SDSS J204749.61−071818.3.....	T0:	20 47 49.61	−07 18 18 3	2000.74	19.70±0.10	16.70±0.03 ^f	15.88±0.03 ^f	15.34±0.03 ^f	1
SDSS J212413.89+010000.3.....	T5	21 24 13.87	+00 59 59 9	2000.63	19.74±0.09	16.03±0.07	16.18±0.20	>16.1	1
2MASS J21392676+0220226.....	T1.5	21 39 26.76	+02 20 22 6	2000.54	...	15.26±0.05	14.17±0.05	13.58±0.05	21
2MASS J21513839−4853542.....	T4	21 51 38.39	−48 53 54 2	1999.72	...	15.73±0.07	15.17±0.10	15.43±0.18	...	0.57±0.07	113	22
ϵ Ind Bab.....	T1/T6 ^m	22 04 10.52	−56 46 57 7	1999.85	...	11.91±0.02	11.31±0.02	11.21±0.02	275.8±0.7	4.7049±0.0010	327	23, 26, 39
2MASS J22282889−4310262.....	T6	22 28 28.89	−43 10 26 2	1998.89	...	15.66±0.07	15.36±0.12	15.30±0.21	...	0.31±0.03	175	7
2MASS J22541892+3123498.....	T4	22 54 18.92	+31 23 49 8	1998.47	...	15.26±0.05	15.02±0.08	14.90±0.15	6
2MASS J23312378−4718274.....	T5	23 31 23.78	−47 18 27 4	2000.79	...	15.66±0.07	15.51±0.15	15.39±0.20	...	0.20±0.07	118	2, 37
2MASS J23391025+1352284.....	T5	23 39 10.25	+13 52 28 4	2000.91	19.42±0.07	16.24±0.11	15.82±0.15	16.15±0.31	...	0.83±0.11	159	6, 19
2MASS J23565477−1553111.....	T5.5	23 56 54.77	−15 53 11 1	1998.54	...	15.82±0.06	15.63±0.10	15.77±0.18	69±3	0.746±0.003	216	6, 24

NOTES.—Units of right ascension are hours, minutes, and seconds, and units of declination are degrees, arcminutes, and arcseconds. Table 14 is also available in machine-readable form in the electronic edition of the *Astrophysical Journal*.

^a If detected in 2MASS, coordinates are from the 2MASS All Sky Point Source Catalog (Cutri et al. 2003), epoch ~1997–2001; otherwise, coordinates are from discovery reference.

^b Unless otherwise noted.

^c NIR spectral type on unified scheme; see § 4.

^d SDSS *z* AB magnitudes from SDSS Data Release 4 (Adelman-McCarthy et al. 2006) or the literature (Leggett et al. 2000; G02; Knapp et al. 2004).

^e Discovery reference given first, followed by references for additional photometric and astrometric data.

^f MKO *JHK* from Leggett et al. (2002b) or Knapp et al. (2004).

^g MKO *JH* photometry from Liu et al. (2002).

^h *JHK* photometry from Zapatero Osorio et al. (2002).

ⁱ Coordinates for GI 229B determined from 2MASS coordinates of GI 229A and offsets from Golimowski et al. (1998).

^j UKIRT *JHK* photometry from Leggett et al. (1999).

^k *JK* photometry from Cuby et al. (1999).

^l Second reference given here is also a discovery reference.

^m Spectral types from resolved spectroscopy (see Table 12).

REFERENCES.—(1) Knapp et al. 2004; (2) Burgasser et al. 2004; (3) Tinney et al. 2005; (4) G02; (5) Liu et al. 2002; (6) B02; (7) Burgasser et al. 2003e; (8) Cruz et al. 2004; (9) Zapatero Osorio et al. 2002; (10) Burgasser et al. 2000b; (11) Nakajima et al. 1995; (12) Leggett et al. 2000; (13) Wilson et al. 2001a; (14) Kirkpatrick et al. 2000; (15) Burgasser et al. 1999; (16) Cuby et al. 1999; (17) Tsvetanov et al. 2000; (18) Burgasser et al. 2000a; (19) Burgasser et al. 2003c; (20) Strauss et al. 1999; (21) K. L. Cruz et al. 2006, in preparation; (22) Ellis et al. 2005; (23) Scholz et al. 2003; (24) Vrba et al. 2004; (25) Leggett et al. 2002b; (26) ESA 1997; (27) Burgasser et al. 2005c; (28) Martín & Zapatero Osorio 2003; (29) Dahn et al. 2002; (30) Oppenheimer et al. 1995; (31) Leggett et al. 1999; (32) McLean et al. 2003; (33) Burgasser et al. 2005b; (34) Nakajima et al. 2001; (35) Reid et al. 2001; (36) A. J. Burgasser et al. 2006, in preparation; (37) Tinney et al. 2003; (38) Burgasser et al. 2003d; (39) McCaughrean et al. 2004.

REFERENCES

- Ackerman, A. S., & Marley, M. S. 2001, *ApJ*, 556, 872
- Adelman-McCarthy, J., et al. 2006, *ApJS*, 162, 38
- Allard, F., Hauschildt, P. H., Alexander, D. R., Tamanai, A., & Schweitzer, A. 2001, *ApJ*, 556, 357
- Bailer-Jones, C. A. L., Coryn A. L., Irwin, M., & von Hippel, T. 1998, *MNRAS*, 298, 361
- Bailer-Jones, C. A. L., & Lamm, M. 2003, *MNRAS*, 339, 477
- Bailer-Jones, C. A. L., & Mundt, R. 1999, *A&A*, 348, 800
- . 2001, *A&A*, 367, 218
- Borysow, A., Jørgensen, U. G., & Zheng, C. 1997, *A&A*, 324, 185
- Bouy, H., Brandner, W., Martin, E. L., Delfosse, X., Allard, F., & Basri, G. 2003, *AJ*, 126, 1526
- Burgasser, A. J., Burrows, A., & Kirkpatrick, J. D. 2005a, *ApJ*, submitted
- Burgasser, A. J., Geballe, T. R., Golimowski, D. A., Leggett, S. K., Kirkpatrick, J. D., Knapp, G. R., & Fan, X. 2003a, in *IAU Symp. 211, Brown Dwarfs*, ed. E. Martín (San Francisco: ASP), 377
- Burgasser, A. J., Kirkpatrick, J. D., Liebert, J., & Burrows, A. 2003b, *ApJ*, 594, 510
- Burgasser, A. J., Kirkpatrick, J. D., & Lowrance, P. J. 2005b, *AJ*, 129, 2849
- Burgasser, A. J., Kirkpatrick, J. D., McElwain, M. W., Cutri, R. M., Burgasser, A. J., & Skrutskie, M. F. 2003c, *AJ*, 125, 850
- Burgasser, A. J., Kirkpatrick, J. D., Reid, I. N., Brown, M. E., Miskey, C. L., & Gizis, J. E. 2003d, *ApJ*, 586, 512
- Burgasser, A. J., Marley, M. S., Ackerman, A. S., Saumon, D., Lodders, K., Dahn, C. C., Harris, H. C., & Kirkpatrick, J. D. 2002a, *ApJ*, 571, L151
- Burgasser, A. J., McElwain, M. W., & Kirkpatrick, J. D. 2003e, *AJ*, 126, 2487
- Burgasser, A. J., McElwain, M. W., Kirkpatrick, J. D., Cruz, K. L., Tinney, C. G., & Reid, I. N. 2004, *AJ*, 127, 2856
- Burgasser, A. J., Reid, I. N., Leggett, S. K., Kirkpatrick, J. D., Liebert, J., & Burrows, A. 2005c, *ApJ*, 634, L177
- Burgasser, A. J., et al. 1999, *ApJ*, 522, L65
- . 2000a, *ApJ*, 531, L57
- . 2000b, *AJ*, 120, 1100
- . 2002b, *ApJ*, 564, 421 (B02)
- Burrows, A., Burgasser, A. J., Kirkpatrick, J. D., Liebert, J., Milsom, J. A., Sudarsky, D., & Hubeny, I. 2002, *ApJ*, 573, 394
- Burrows, A., Sudarsky, D., & Lunine, J. I. 2003, *ApJ*, 596, 587
- Cannon, A. J., & Pickering, E. C. 1918a, *Ann. Astron. Obs. Harvard Coll.*, 91, 1
- . 1918b, *Ann. Astron. Obs. Harvard Coll.*, 92, 1
- . 1919a, *Ann. Astron. Obs. Harvard Coll.*, 93, 1
- . 1919b, *Ann. Astron. Obs. Harvard Coll.*, 94, 1
- . 1920, *Ann. Astron. Obs. Harvard Coll.*, 95, 1
- . 1921, *Ann. Astron. Obs. Harvard Coll.*, 96, 1
- . 1922, *Ann. Astron. Obs. Harvard Coll.*, 97, 1
- . 1923, *Ann. Astron. Obs. Harvard Coll.*, 98, 1
- . 1924, *Ann. Astron. Obs. Harvard Coll.*, 99, 1
- Corbally, C. J., Gray R. O., & Garrison, R. F., eds. 1994, *The MK Process at 50 Years. A Powerful Tool for Astrophysical Insight* (San Francisco: ASP)
- Cruz, K. L., Burgasser, A. J., Reid, I. N., & Liebert, J., 2004, *ApJ*, 604, L61
- Cruz, K. L., Reid, I. N., Liebert, J., Kirkpatrick, J. D., & Lowrance, P. J. 2003, *AJ*, 126, 2421
- Cuby, J. G., Saracco, P., Moorwood, A. F. M., D'Odorico, S., Lidman, C., Comerón, F., & Spyromilio, J. 1999, *A&A*, 349, L41
- Cushing, M. C., Rayner, J. T., & Vacca, W. D. 2005, *ApJ*, 623, 1115
- Cushing, M. C., Vacca, W. D., & Rayner, J. T. 2004, *PASP*, 116, 362
- Cutri, R. M., et al. 2003, *Explanatory Supplement to the 2MASS All Sky Data Release*, <http://www.ipac.caltech.edu/2mass/releases/allsky/doc/explsup.html>
- Dahn, C. C., et al. 2002, *AJ*, 124, 1170
- Delfosse, X., Tinney, C. G., Forveille, T., Epchtein, N., Borsenberger, J., Fouqué, P., Kimeswenger, S., & Tiphène, D. 1999, *A&AS*, 135, 41
- Delfosse, X., et al. 1997, *A&A*, 327, L25
- Depoy, D. L., Atwood, B., Byard, P. L., Frogel, J., & O'Brien, T. P. 1993, *Proc. SPIE*, 1946, 667
- Ellis, S. C., Tinney, C. G., Burgasser, A. J., Kirkpatrick, J. D., & McElwain, M. W. 2005, *AJ*, 130, 2347
- Enoch, M. L., Brown, M. E., & Burgasser, A. J. 2003, *AJ*, 126, 1006
- Epchtein, N., et al. 1997, *Messenger*, 87, 27
- ESA 1997, *The Hipparcos and Tycho Catalogues* (ESA SP-1200; Noordwijk: ESA)
- Fukugita, M., Ichikawa, T., Gunn, J. E., Doi, M., Shimasaku, K., & Schneider, D. P. 1996, *AJ*, 111, 1748
- Garrison, R. F., ed. 1984, *The MK Process and Stellar Classification: Proceedings of the Workshop in Honour of W. W. Morgan and P. C. Keenan* (Toronto: David Dunlap Obs.)
- Geballe, T. R., Kulkarni, S. R., Woodward, C. E., & Sloan, G. C. 1996, *ApJ*, 467, L101
- Geballe, T. R., Saumon, D., Leggett, S. K., Knapp, G. R., Marley, M. S., & Lodders, K. 2001, *ApJ*, 556, 373
- Geballe, T. R., et al. 2002, *ApJ*, 564, 466 (G02)
- Gelino, C. R., Marley, M. S., Holtzman, J. A., Ackerman, A. S., & Lodders, K. 2002, *ApJ*, 577, 433
- Gizis, J. E. 1997, *AJ*, 113, 806
- Golimowski, D. A., Burrows, C. S., Kulkarni, S. R., Oppenheimer, B. R., & Brukardt, R. A. 1998, *AJ*, 115, 2579
- Golimowski, D. A., et al. 2004, *AJ*, 127, 3516
- Griffith, C. A., & Yelle, R. V. 2000, *ApJ*, 532, L59
- Griffith, C. A., Yelle, R. V., & Marley, M. S. 1998, *Science*, 282, 2063
- Hayashi, C., & Nakano, T. 1963, *Prog. Theor. Phys.*, 30, 4
- Helling, C., Klein, R., Woitke, P., Nowak, U., & Sedlmayr, E. 2004, *A&A*, 423, 657
- Helling, C., Oevermann, M., Lüttke, M. J. H., Klein, R., & Sedlmayr, E. 2001, *A&A*, 376, 194
- Houk, N. 1978, *Michigan Catalogue of Two-Dimensional Spectral Types for the HD Stars, Vol. 2: Declinations -53 to -40 Degrees* (Ann Arbor: Univ. Michigan)
- . 1982, *Michigan Catalogue of Two-Dimensional Spectral Types for the HD Stars, Vol. 3: Declinations -40 to -26 Degrees* (Ann Arbor: Univ. Michigan)
- Houk, N., & Cowley, A. P. 1975, *Michigan Catalogue of Two-Dimensional Spectral Types for the HD Stars, Vol. 1: Declinations -90 to -53 Degrees* (Ann Arbor: Univ. Michigan)
- Houk, N., & Smith-Moore, M. 1988, *Michigan Catalogue of Two-Dimensional Spectral Types for the HD Stars, Vol. 4: -26 to -12 Degrees* (Ann Arbor: Univ. Michigan)
- Houk, N., & Swift, C. 1999, *Michigan Catalogue of Two-Dimensional Spectral Types for the HD Stars, Vol. 5* (Ann Arbor: Univ. Michigan)
- Hubble, E. 1936, *The Realm of the Nebulae* (New Haven: Yale Univ. Press)
- Jones, H. R. A., Longmore, A. J., Allard, F., & Hauschildt, P. H. 1996, *MNRAS*, 280, 77
- Jones, H. R. A., Longmore, A. J., Jameson, R. F., & Mountain, C. M. 1994, *MNRAS*, 267, 413
- Keenan, P. C., & McNeil, R. C. 1976, *An Atlas of Spectra of the Cooler Stars: Types G, K, M, S and C* (Columbus: Ohio State Univ. Press)
- Kirkpatrick, J. D., et al. 1999, *ApJ*, 519, 802
- . 2000, *AJ*, 120, 447
- Knapp, G., et al. 2004, *AJ*, 127, 3553
- Kobayashi, N., et al. 2000, *Proc. SPIE*, 4008, 1056
- Koen, C. 2003, *MNRAS*, 346, 473
- . 2004, *MNRAS*, 354, 378
- Kumar, S. S. 1962, *AJ*, 67, 579
- Leggett, S. K., Hauschildt, P. H., Allard, F., Geballe, T. R., & Baron, E. 2002a, *MNRAS*, 332, 78
- Leggett, S. K., Toomey, D. W., Geballe, T. R., & Brown, R. H. 1999, *ApJ*, 517, L139
- Leggett, S. K., et al. 2000, *ApJ*, 536, L35
- . 2002b, *ApJ*, 564, 452
- Lenzen, R., et al. 1998, *Proc. SPIE*, 3354, 606
- Linnaeus, C. 1735, *Systema Naturae*
- Liu, M. C., Wainscoat, R., Martín, E. L., Barris, B., & Tonry, J. 2002, *ApJ*, 568, L107
- Lodders, K. 2002, *ApJ*, 577, 974
- Lupton, R. H., Gunn, J. E., & Szalay, A. S. 1999, *AJ*, 118, 1406
- Martin, E. L., Delfosse, X., Basri, G., Goldman, B., Forveille, T., & Zapatero Osorio, M. R. 1999, *AJ*, 118, 2466
- Martin, E. L., & Zapatero Osorio, M. R. 2003, *ApJ*, 593, L113
- Matthews, K., & Soifer, B. T. 1994, in *Infrared Astronomy with Arrays: The Next Generation*, ed. I. McLean (Dordrecht: Kluwer), 239
- McCaughrean, M., Close, L. M., Scholz, R.-D., Lenzen, R., Biller, B., Brandner, W., Hartung, M., & Lodieu, N. 2004, *A&A*, 413, 1029
- McLean, I. S., Graham, J. R., Becklin, E. E., Figer, D. F., Larkin, J. E., Levenson, N. A., & Teplitz, H. I. 2000, *Proc. SPIE*, 4008, 1048
- McLean, I. S., McGovern, M. R., Burgasser, A. J., Kirkpatrick, J. D., Prato, L., & Kim, S. 2003, *ApJ*, 596, 561
- McLean, I. S., et al. 1998, *Proc. SPIE*, 3354, 566
- Mendeleev, D. 1869, *Zeitschrift für Chemie*, 12, 405
- Mohanty, S., Basri, G., Shu, F., Allard, F., & Chabrier, G. 2002, *ApJ*, 571, 469
- Moorwood, A. F. 1997, *Proc. SPIE*, 2871, 1146
- Moorwood, A. F., Cuby, J.-G., & Lidman, C. 1998, *Messenger*, 91, 9
- Morgan, W. W., Abt, H. A., & Tapscott, J. W. 1978, *Revised MK Spectral Atlas for Stars Earlier than the Sun* (Williams Bay: Yerkes Obs.; Tucson: KPNO)
- Morgan, W. W., & Keenan, P. C. 1973, *ARA&A*, 11, 29
- Morgan, W. W., Keenan, P. C., & Kellman, E. 1943, *An Atlas of Stellar Spectra, with an Outline of Spectral Classification* (Chicago: Univ. Chicago Press)

- Morgan, W. W., Sharpless, S., & Osterbrock, D. 1952, *AJ*, 57, 3
- Motohara, K., et al. 2002, *PASJ*, 54, 315
- Nakajima, T., Oppenheimer, B. R., Kulkarni, S. R., Golimowski, D. A., Matthews, K., & Durrance, S. T. 1995, *Nature*, 378, 463
- Nakajima, T., Tsuji, T., Tamura, M., & Yamashita, T. 2000, *PASJ*, 52, 87
- Nakajima, T., Tsuji, T., & Yanagisawa, K. 2001, *ApJ*, 561, L119
- . 2004, *ApJ*, 607, 499
- Oppenheimer, B. R., Kulkarni, S. R., Matthews, K., & Nakajima, T. 1995, *Science*, 270, 1478
- Oppenheimer, B. R., Kulkarni, S. R., Matthews, K., & van Kerkwijk, M. H. 1998, *ApJ*, 502, 932
- Rayner, J. T., Toomey, D. W., Onaka, P. M., Denault, A. J., Stahlberger, W. E., Vacca, W. D., Cushing, M. C., & Wang, S. 2003, *PASP*, 115, 362
- Reid, I. N., Burgasser, A. J., Cruz, K., Kirkpatrick, J. D., & Gizis, J. E. 2001, *AJ*, 121, 1710
- Reid, I. N., Hawley, S. L., & Gizis, J. E. 1995, *AJ*, 110, 1838
- Roellig, T. L., et al. 2004, *ApJS*, 154, 418
- Rountree, J., & Sonneborn, G. 1991, *ApJ*, 369, 515
- Saumon, D., Bergeron, P., Lunine, J. I., Hubbard, W. B., & Burrows, A. 1994, *ApJ*, 424, 333
- Scholz, R.-D., McCaughrean, M. J., Lodieu, N., & Kuhlbrodt, B. 2003, *A&A*, 398, L29
- Secchi, A. 1866, *CR Acad. Sci. Paris*, 63, 621
- Simons, D. A., & Tokunaga, A. T. 2002, *PASP*, 114, 169
- Stephens, D. C., & Leggett, S. K. 2004, *PASP*, 116, 9
- Strauss, M. A., et al. 1999, *ApJ*, 522, L61
- Testi, L., et al. 2001, *ApJ*, 552, L147
- Tinney, C. G., Burgasser, A. J., & Kirkpatrick, J. D. 2003, *AJ*, 126, 975
- Tinney, C. G., Burgasser, A. J., Kirkpatrick, J. D., & McElwain, M. W. 2005, *AJ*, 130, 2326
- Tinney, C. G., Delfosse, X., Forveille, T., & Allard, F. 1998, *A&A*, 338, 1066
- Tinney, C. G., & Tolley, A. J. 1999, *MNRAS*, 304, 119
- Tokunaga, A. T., & Kobayashi, N. 1999, *AJ*, 117, 1010
- Tokunaga, A. T., Simons, D. A., & Vacca, W. D. 2002, *PASP*, 114, 180
- Tsuji, T. 2005, *ApJ*, 621, 1033
- Tsuji, T., & Nakajima, T. 2003, *ApJ*, 585, L151
- Tsuji, T., Ohnaka, K., Aoki, W., & Nakajima, T. 1996, *A&A*, 308, L29
- Tsvetanov, Z. I., et al. 2000, *ApJ*, 531, L61
- Vacca, W. D., Cushing, M. C., & Rayner, J. T. 2003, *PASP*, 115, 389
- von Hippel, T., Storrer-Lombardi, L. J., Storrer-Lombardi, M. C., & Irwin, M. J. 1994, *MNRAS*, 269, 97
- Vrba, F. J., et al. 2004, *AJ*, 127, 2948
- Wallace, L., & Hinkle, K. 1997, *ApJS*, 111, 445
- Warren, S. 2002, *Proc. SPIE*, 4836, 313
- Wilson, J. C., et al. 2001a, *AJ*, 122, 1989
- . 2001b, *PASP*, 113, 227
- Woitke, P., & Helling, C. 2003, *A&A*, 399, 297
- . 2004, *A&A*, 414, 335
- Wright, G. S., Mountain, C. M., Bridger, A., Daly, P. N., Griffin, J. L., & Ramsay-Howat, S. K. 1993, *Proc. SPIE*, 1946, 547
- York, D. G., et al. 2000, *AJ*, 120, 1579
- Zapatero Osorio, M. R., Béjar, V. J. S., Martí, E. L., Rebolo, R., Barrado y Navascués, D., Mundt, R., Eisloffel, J., & Caballero, J. A. 2002, *ApJ*, 578, 536